UNIVERSITÀ DEGLI STUDI DI PADOVA

Dipartimento di Ingegneria Industriale DII

Corso di Laurea in Ingegneria Aerospaziale

Relazione per la prova finale

Technological Advancements in Military Aero-Engines

Tutor Universitario: Prof. Ernesto Benini

Alessandro Azzano

Anno Accademico 2023/2024

Ringraziamenti

Oggi si conclude un grande capitolo della mia vita, forse il più importante. È stato un percorso lungo, faticoso, in cui mi sono perso e ritrovato più volte. Sono arrivato alla fine solo grazie a tutte le persone che ho avuto al mio fianco e che mi vogliono bene, e sono felice di condividere con voi questo fantastico obiettivo.

Vorrei ringraziare il mio relatore, il professor Ernesto Benini, per avermi accompagnato nel percorso della scrittura della tesi.
Per me è stato un vero e proprio mentore. È riuscito a trasmettermi tutta la sua passione e a farmi innamorare della sua materia. I suoi discorsi sono sempre stati ispirazionali e ha sempre avuto una parola gentile per me.
Averlo conosciuto è stato un tassello fondamentale per raggiungere questo traguardo.

Index

Introduction

The evolution of military fighter jets has been marked by substantial advancements from the 4th to the 5th generation. These advancements represent significant leaps in performance, efficiency, and operational capability.
The engines powering modern fighter jets have undergone notable enhancements in thrust, fuel efficiency, reliability, and maintainability. This progress has been driven by cutting-edge technologies in materials science, digital control systems and innovative engineering concepts. This thesis aims to provide a comprehensive analysis of these advancements, focusing on characteristics and technological developments of the primary western fighter jet engines currently in service.

The study begins with an examination of the 4th generation fighter jet engines, which were designed with a strong emphasis on improving maneuverability, multi-role capabilities and avionics integration. Key engines, such as the F-100-PW-229 used in the F-15 Eagle and F-16 Fighting Falcon, and the EJ-200 powering the Eurofighter Typhoon serve as case studies to illustrate these differences from the 3rd generation engines.

Moving forward, this dissertation explores the 5th generation fighter jet engines, which further develops these improvements and introduces new technologies to achieve superior stealth, performance, and adaptability. Engines like the Pratt & Whitney F-119-PW-100 and F-135-PW-100 are the pinnacle of the state-of-the-art technology available. Key features of this generation of military aircraft include advanced materials, sophisticated digital controls, and innovative design concepts such as the Minimum Length Nozzle, the Diverterless Supersonic Inlet and the Low Observable Axisymmetric Nozzle.

A significant portion of this thesis is dedicated to the Adaptive Cycle Engine (ACE), a revolutionary development in fighter jet engine technology. The ACE represents the next frontier in propulsion systems, offering the ability to switch between different cycles to optimize performance across various flight conditions. This innovative system promises substantial benefits in terms of fuel efficiency, thrust, and overall mission effectiveness.
The main focus of this dissertation is to study and analyze the origins, technological principles and potential future applications of the ACE. Comparing the revolutionary ACE to traditional fixed-geometry turbofans, this work tried to evaluate the real benefits of adopting this high-risk technology for future military jets, attempting to answer the fundamental questions "Is it worth it? Considering its feasibility, what are the real advantages and how convenient it is".

1 Characteristics of 4th and 5th Generation Fighter Jet Engines

4$^{\text{th}}$ and 5$^{\text{th}}$ generation fighters are the planes in service nowadays. The engines in these aircraft have undergone significant improvements delivering better performance and also decreasing operational and service costs, widening the lifespan and simplifying maintenance. These improvements come from the discoveries of new technologies in various fields, such as materials, digital controls, evolution in engine concepts and innovative ideas.

In this chapter we will analyze the main features of state-of-the-art principal occidental engines and their evolution throughout the years.

1.1 4$^{\text{th}}$ Generation Fighters

4$^{\text{th}}$ generation fighters are heavily influenced by lessons learned from the previous generation of combat aircraft [1]. 3$^{\text{rd}}$ generation fighters were primarily designed as interceptors, therefore focusing around speed and air superiority. 3$^{\text{rd}}$ gen fighter jets were exceptionally fast in a straight line, albeit many of them lack in maneuverability. As a result of this, they were poor in dogfights since it's common knowledge that agility is more important than speed in air-to-air combat.

Moreover, air-to-air missiles at the time, despite being responsible for the vast majority of air-to-air victories, were quite unreliable, and combat would quickly become subsonic and would result in close-range encounters. This would have left fighter jets of the time vulnerable, inspiring the increase in manoeuvrability for the fourth generation of fighters.

Meanwhile, the growing costs of military aircraft and the demonstrated success of aircraft such as the McDonnell Douglas F-4 Phantom II gave rise to the popularity of multi-role military aircraft in parallel with the development of fourth generation. Important innovations were also introduced in avionics systems such as fly-by-wire and digital control for every system of the aircraft.

1.1.1 The F-100-PW-229 for F-15 Eagle and F-16 Fighting Falcon

The F-100-PW-100 originated from Initial Engine Development Program (IEDP). It was being developed throughout the years to reach the final F-100-PW-229, which with the EMD (Engine Model Derivative) reached higher inlet turbine temperature, lower bypass ratio, more airflow and it brought with it improvements in reliability and durability.

It has a maximum dry power of 79.2 kN and an augmented maximum power of 129.7 kN [2].
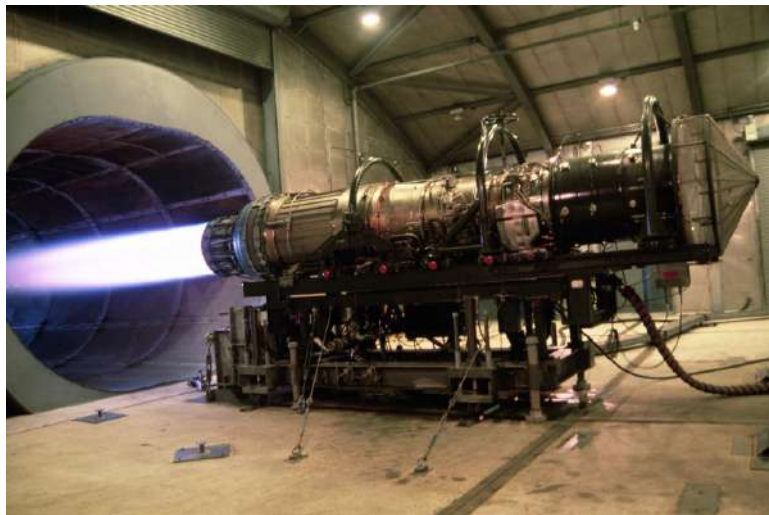
Figure 1: *The F-100-PW-229 engine [3]*

The F-100 is a twin-spool low-bypass (0.36) turbofan.

It is composed of a three-stage fan behind an integral anti-iced vane frame with struts and variable inlet guide vanes, that can cover and protect the engine from potential debris.

The compressor was initially made by nine stages, albeit to increase pressure ratios and flow one more stage was added, making a ten-stage High-Pressure Compressor. To facilitate maintenance all the blades are replaceable. The compressor rotor is internally convectively cooled with the third-stage compressor air, which is vented aft to cool the Low-Pressure

Turbine rotor as well.

The combustor uses a Float-Wall technology which leads to a shorter part that can reach higher temperature and therefore reaching more performance.

The High-Pressure Turbine has minimum stress concentrations and no bolt or cooling holes in the disks webs. A single-crystal material was used to improve durability and heat resistance.

The Low-Pressure Turbine was developed to match the increased power fan. To do this it features a larger flow area and improved seals and shrouds. The turbine has two stages that are relatively lightly aerodynamically loaded. The work is split in a 70/30 ratio between the first and second stage, with the first stage being cooled due to the higher temperatures.

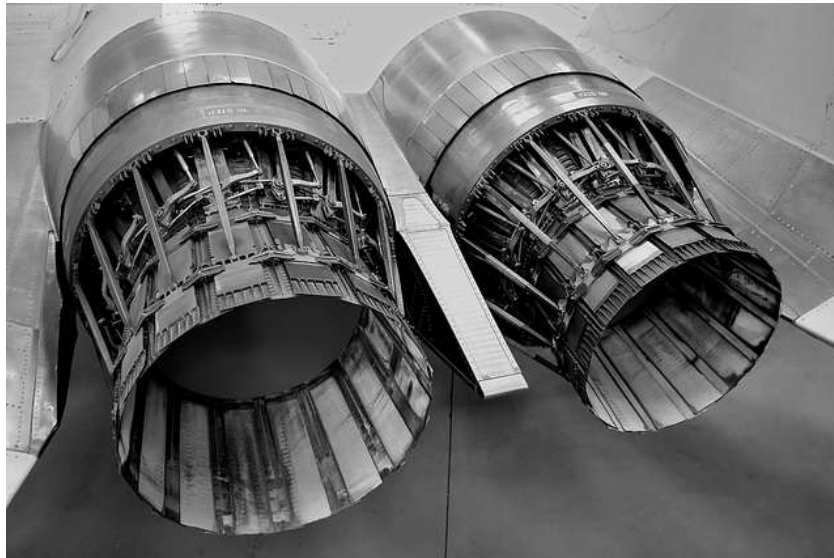The nozzle is a convergent-divergent adaptable nozzle adjustable to adapt at different flight conditions.

Figure 2: *The F-100-PW-229 and its nozzle [3]*

1.1.2 The EJ-200 for the Eurofighter Typhoon

EJ-200 is the engine developed by EuroJet Turbo GmbH consortium formed by Rolls-Royce for the United Kingdom, Avio for Italy, Industria de Turbo Propulsores (ITP) for Spain and MTU Aero Engines for Germany.
It's a low-bypass (0.4) twin-spool turbofan, smaller in size and weight but still with a maximum dry thrust of 60 kN and augmented thrust of 89 kN [4].

The Low-Pressure Compressor is composed of three fan built with blisk (bladed disk) technology, which means that the rotor disk and the blades are a single part (rather than a disk assembled with individual removable blades), with better aerodynamics and less weight if compared to traditional builds [5].

The first three of five stages of the High-Pressure Compressor are built with blisk technology as well. There's just one stator row in the HPC which has a variable angle of incidence.

Both the High-Pressure and Low-Pressure Turbine are single-staged. They are built with a single-crystal nickel alloy. The blades are cooled both internally and externally with compressed air coming from the HPC flowing through holes made on the blade. Moreover, on stators and sidewalls of the internal ducts a plasma flow is applied to work as a thermal protection barrier [6].

Figure 3: *The EJ-200 engine [7]*

The augmenter is not an annular one as for the other engines. The flame stabilizers are axial instead, this is because the high temperatures of the exhaust gasses coming out from the Low-Pressure Turbine are still too high, therefore it is necessary to cool the flame stabilizers through the cold flow coming from the bypass stream. Furthermore, some screech dampers are installed in the afterburner to reduce the noise created in the engine and to protect the nozzle from overheating.

The EFA's convergent-divergent nozzle is a variable geometry nozzle which can be adapted to the very different conditions in terms of airflow and temperatures that the nozzle can encounter throughout the flight envelop of a fighter jet. The convergent part consists of a series of primary petals hinged at one end to the engine structure and, at the other end (corresponding to the throat section), to the secondary petals. A ring moved by hydraulic actuators controls the movement of the secondary petals which, constrained to the primary ones, open or close, regulating both the throat section and the divergence of the nozzle.

A version of the EJ-200 with Thrust Vectoring Nozzle (TVN) has been under study. The system involves three rings hinged together to form a gimbal joint between the engine and the exhaust nozzle. The basic configuration involves the use of three actuators mounted at 120° intervals which, by moving the gimbal joint in a coordinated manner, focuses the thrust in the desired direction.

Figure 4: *The EJ-200's nozzle [7]*

1.2 5th Generation Fighters

A 5th generation fighter is a classification of jet fighter aircraft that incorporates advanced technologies defining the capabilities of modern and future combat aircraft [8]. While there is no universal agreement on the characteristics of fifth-generation fighters, they generally include features such as stealth, low-probability-of-intercept radar, agile airframes with supercruise performance, advanced avionics, and highly integrated computer systems. These systems are capable of networking with other components within the battle-space, enhancing situational awareness, and providing superior command, control, and communications capabilities.

1.2.1 The Pratt & Whitney F-119-PW-100 for the F-22 Raptor

The Lockheed Martin F-22 Raptor is a low-observable, data fusion, enhanced manoeuvrability, capable of high levels of agility and supercruise (sustained supersonic flight without afterburner) air-dominance aircraft [9]. To achieve these characteristics, it is equipped with two Pratt & Whitney F-119 engines.
The F-119 is an afterburning low-bypass turbofan engine developed from its predecessor, the F-100.
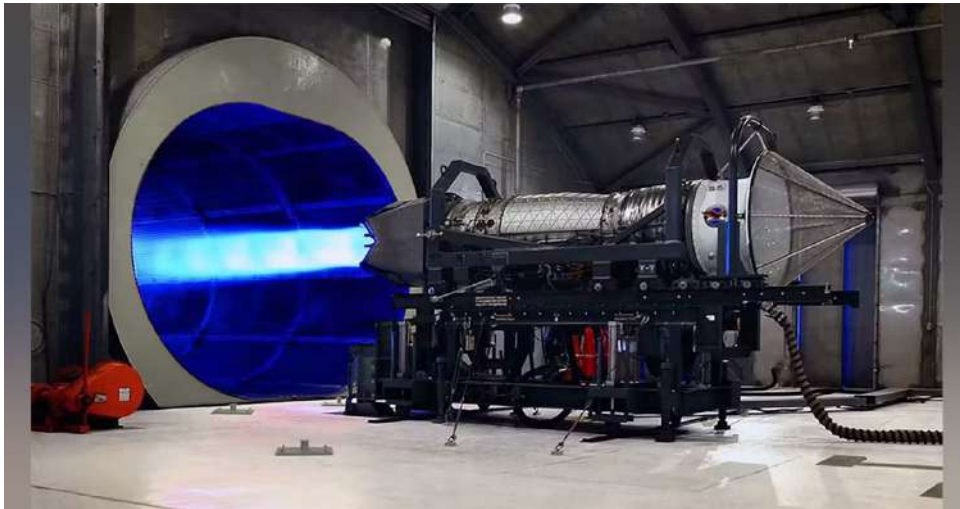

Figure 5: *The Pratt & Whitney F-119 being tested [9]*

As part of the U.S. Air Force's Advanced Tactical Fighter (ATF) program, the Advanced Technology Fighter Engine (ATFE) program was intended to provide the most advanced, cost-effective and mission-effective powerplant for next generation USAF fighter aircraft.
Goals of the ATFE project were initially set as:

- STOL, Short Take-Off and Landing capability

- Stealth characteristics, including reduced infrared and radar signatures

- Reduction in life-cycle costs of at least 25% throughout improvements in parts life and reduction in parts count from former engines

- Increase in thrust to weight ratio of 20%

- Supercruise, which means that the aircraft should be able to sustain supersonic speed without using afterburners

- A reduction of 30 to 50% in fuel flow at dry supersonic cruise thrust, which would translate in a reduction of 8 to 10% in SFC

The performance required to achieve these objectives were ambitious, as was the F-22 project. A big step forward was required for the development of the engine.
The outcome was a low-bypass turbofan with a bypass ratio of 0.30:1, which is the minimum determined by the required afterburning ratio and the need to cool the afterburner [10]. It lies in the 35,000 lbst class (155.6 kN) with full augmentation and it has 22,000 lbst (98.8 kN) maximum dry thrust.

It also features digital electronic engine control, called FADEC (Full Authority Digital Engine Control).
FADEC [11] is a computer-managed aircraft ignition and engine control system used to manage all aspects of engine

performance digitally, instead of using technical or analog electronic controls. It reacts to pilot inputs, but it also uses data from sensors to automatically adjust engine settings to optimize performance. Since this kind of system is digital, it also brings benefits in terms of major weight reduction and easier maintenance compared to older control systems.

The use of advanced technology in materials was widespread throughout the engine.
In particular for the burner a new technology called Float-Wall was implemented to build a shingled combustor, a single, fully annular combustor with isolated panels of oxidization-resistant cobalt material. Static hot section parts in the combustor are made of ceramic or carbon/carbon materials with ceramic material turbine high-pressure seals.
Single-crystal blades and vanes are used in the turbine sections. In this engine were also experimented the use of HIP-ed powder metal and eutectic materials.

The F-119 is a twin-spool turbofan incorporating advanced materials, with a much lower parts and stage count (3 (3(FAN)+6(HPC)+1(HPT)+1(LPT)) than its F-100 predecessor (3+10+2+2).
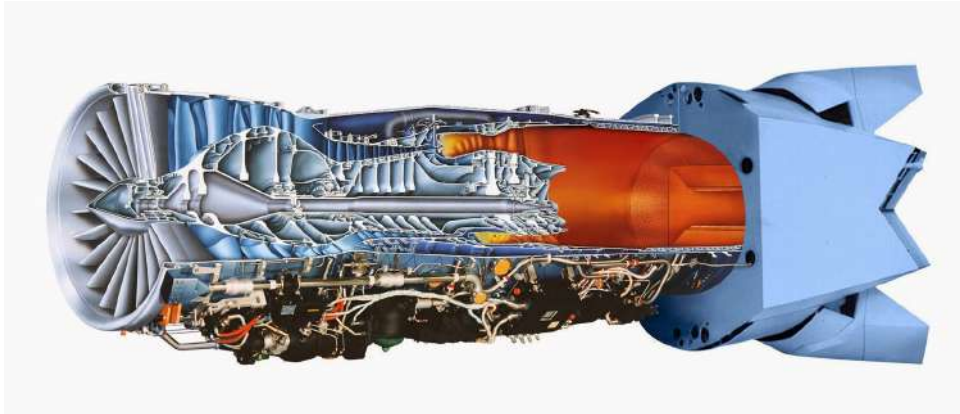

Figure 6: *The Pratt & Whitney F-119 scheme [10]*

- **Fan**: it's a three stage fan with an estimated π_{fan} of 4. It is diffusion bonded from machined titanium halves, which are linear friction welded to the disk

- **High-Pressure Compressor**: it's a six stage compressor with an overall π_{tot} of 35. It is completed with alloy C titanium compressor stators

- **High-Pressure Turbine**: a single-stage turbine with single-crystal blades

- **Low-Pressure Turbine**: this is also a single-stage turbine which rotates in the opposite direction of the HPT, which brings benefits to the weight since it's possible to remove one row of stators

The three-zone afterburner contributes to the stealth of the aircraft by having fuel injectors integrated into thick curved vanes coated with ceramic Radar-Absorbent Materials (RAM). These vanes replace the traditional fuel spray bars, flame holders, and block line-of-sight of the turbines.

The nozzle systems is composed of a two-dimensional vectoring convergent-divergent nozzle. The vectors thrust 20° up and down with the help of precision digital controls, working like another flight control surface. The nozzle is an integrated part of the advanced F-22 flight control system which allows a total integration of all aircraft components. This additional control system increases the roll rate of the plane by 50%.
Alloy C and graphite-polymide are used as building materials. Heat-resistant components give the nozzles the durability needed to vector thrust, even in afterburner conditions.

Figure 7: *The 2D MLN rectangular nozzle of the F-22 Raptor [9]*

To provide thrust vectoring, using a circular nozzle would produce slightly more thrust from the same engine rather than a rectangular nozzle.

The reason why this type of nozzle is used [12] is its superior capability of mixing in the shear layer trailing the nozzle. Therefore the hot exhaust from the jet is able to mix quicker with with cool ambient air, which results in significantly lower heat signature of the aircraft.

This process is essential to increase thermal stealth capabilities and to maximize noise reduction. The latter also results in better stealth characteristics due to the improvements in noise tracking systems.

There are also advantages in terms of dimensions: the Minimum Length Nozzle (MLN), with a rectangular cross section, is 30% shorter than standard circular nozzle.

Another important element is serpentine inlet. Due to the shape of this kind of supersonic inlet, the compressors blades are hidden. The S-inlet, together with the use of RAM (Radar Absorbent Material), contribute to make the stealth capabilities of the Raptor so revolutionary.
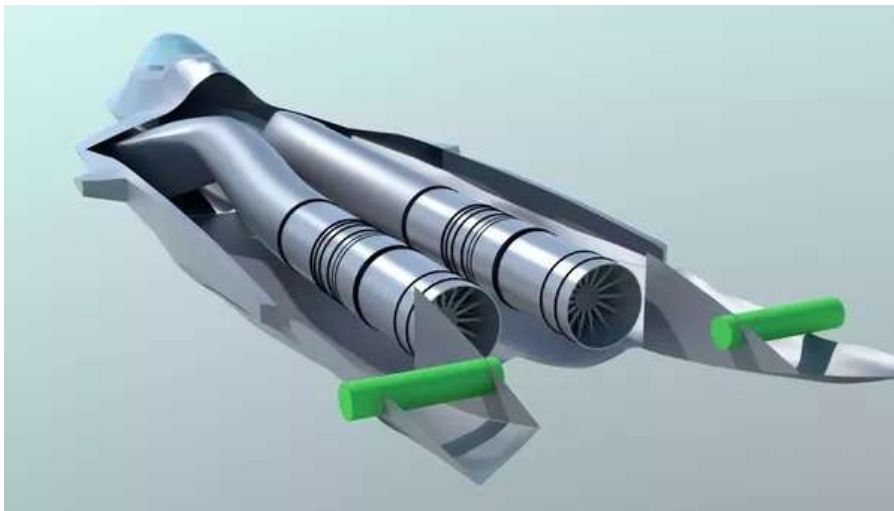
Figure 8: *The F-22 innovative serpentine-duct intake [9]*

The F-22's inlets are different from the DSI of the F-35 (that we will further analyze later in the chapter). These are called caret inlets. They have a triangular or diamond-shaped cross-section [13].

They use a series of external ramps or wedges to create shock waves that slow down and compress incoming air before it enters the engine. For Boundary Layer Control, they feature diverters or bleed systems to separate and remove the slower-moving boundary layer air from the intake flow, preventing it from entering the engine and causing performance issues.

They are mechanically complex and not optimal in terms of costs and weight, albeit they can reach high performance.

Figure 9: *The Caret inlets particular of a F-22 Raptor [9]*

1.2.2 The Pratt & Whitney F-135-PW-100 for the F-35 Lightning II

The Lockheed Martin F-35 Lightning II is a true 5th generation tri-variant, all-weather, stealth, multi-role combat aircraft designed to be not only a fighter, but also a multi-service air system. Beyond its main tasks, which are strike missions and air superiority, the F-35 stands out also in electronic warfare and intelligence, surveillance and reconnaissance missions, which makes the Lightning II the perfect definition of multi-role aircraft.
It was born from the JSF (Joint Strike Fighter) program.

Figure 10: *The F-135-PW-100, powering the F-35A [14]*

F-35 is a single-engine aircraft, powered by a PW F-135. Since the aircraft has three variants, the engine has three variants as well.

- **CTOL**: Conventional Take-Off and Landing, F-35A, uses the classic F-135-PW-100 (it's the engine we are going to study)

- **STOVL**: Short Take-Off and Vertical landing, F-35B, uses the F-135-PW-600. It has a two stage lift fan on the front of the aircraft powered by the main engine which generate enough lift to accomplish a vertical landing (vertical

takeoff is also possible, but it's preferred to do a short takeoff instead). This model is deployed on small to medium size aircraft carrier

- **STOL**: Short Take-Off and Landing, F-35C, uses the F-135-PW-400, a slightly modified version of the PW-100 for what concerns salt-resistant materials, deployed on large-size aircraft carrier (with catapults)

The main advantages of this aircraft is to share the main platform for both the plane and the engine, reducing production and development costs.

Figure 11: *F-135-PW-600, the VTOL version with the lift fan [14]*

The F-135 is a mixed-flow afterburning turbofan developed from its predecessor, the F-119.
It lies in the 43,000 lbf class (191 kN) augmented and 28,000 lbf (125 kN) in dry conditions [15]. It has a larger fan system, a higher bypass ratio of about 0.57 and a more powerful Low-Pressure Turbine (it's composed of two stages, one more than its predecessor) if compared to the F-119. This has been done to increase subsonic thrust and fuel efficiency, while sacrificing the supersonic thrust: as a matter of fact the F-35 does not possess supercruise capabilities [16].
The F-35 can cruise without afterburners at a transonic speed of Mach 1.1 for 150 miles.

Like the F-119, the F135 has a stealthy augmenter where traditional spray bars and flame-holders are replaced by thick curved vanes coated with ceramic RAM (Radar-Absorbent Materials). Afterburner fuel injectors are integrated into these vanes, which block line-of-sight of the turbines, contributing to aft-sector stealth.

The engine has fewer parts, which leads to reduce costs and easier maintenance and troubleshooting.

1.2.3   Diverterless Supersonic Inlet

The F-135 main air induction system features a twin couple of Diverterless Supersonic Inlet (DSI) characterized by a 3-D compression surface and a forward-swept cowl [17]. These two components together allows high aerodynamic performance, boundary layer diversion and inlet stability without the necessity to use a boundary layer diverter or bleed system, which leads to reduction of weight and costs and an increase in stealth capabilities.
Two different requirements had been considered to design this system:

- **Flow Compression**: the airstream speed needs to be reduced while the static pressure should increase. In the past, in combat aircraft, this was done with a series of external shock waves and internal flow area expansion.

- **Boundary Layer Control** (BLC): this must be taken into account at both subsonic and supersonic speeds, since the interaction between shock waves and boundary layer can lead to severe airflow distortion which may cause the stall of the engine. To deal with BLC it is possible to physically separate the inlet from the fuselage with a boundary layer diverter; another technique is boundary layer bleed, which can be fixed or involve mechanical actuators to improve performance. Many of today's aircraft use a combination of both these solutions
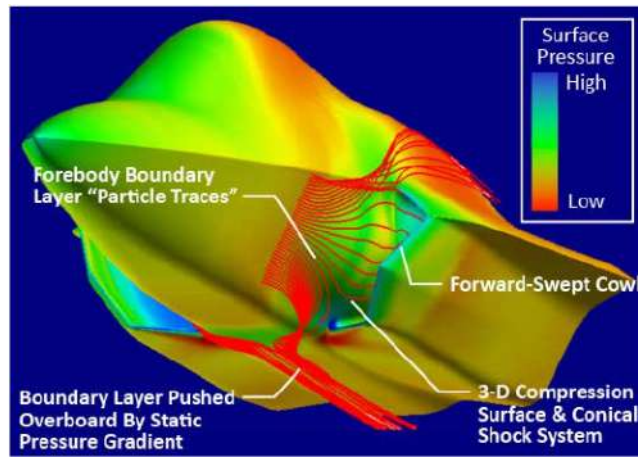
Figure 12: CFD simulation of DSI supersonic Boundary Layer Diversion [16]

As said above, the innovation for the inlet system was to remove these solutions and install a DSI instead.

The bump (3-D fixed) compression surface derives from the flow field produced by a reference axisymmetric body in supersonic flow. A set of CFD particle traces are released along a set of points representing the intersection of of the shock field and aircraft surface.

As the particles travel into the shock field, they are deflected away from our reference body, a virtual cone, by internal flow filed pressure gradients. A 3-D contour is defined by a surface smoothly shaped through the particle traces.

The bump contributes to flow compression and creates a span-wise static pressure gradient that helps with boundary layer diversion.

Thanks to the forward-swept cowl geometry low-pressure boundary layer air is spilled out to the side of the inlet as mass flow ratio is reduced.

The latter together with the bump compression surface can substitute more traditional inlets reducing weight, mechanical complexity and costs.

Sure enough, after many tests both on small-scale models and on actual aircraft, a 30% inlet weight reduction was estimated for the DSI compared to the reference caret inlet, a more classical system used on F-22 or F-18. Most of this weight reduction was attributed to the removal of the bleed and bypass system.

1.2.4   Low Observable Axisymmetric Nozzle

For the Lightning II, the ability to see before being seen was the main objective, therefore Low Observability (LO) was a primary goal.

LOAN (Low Observable Axisymmetric Nozzle) was an innovative nozzle compared to the previous with fixed high aspect ratio designs or heavy two-dimensional systems. This new technology was capable of balancing the requirements of LO with efficient aero-mechanical performance.

It is composed of fifteen partially overlapping flaps creating a sawtooth pattern at the trailing edge.
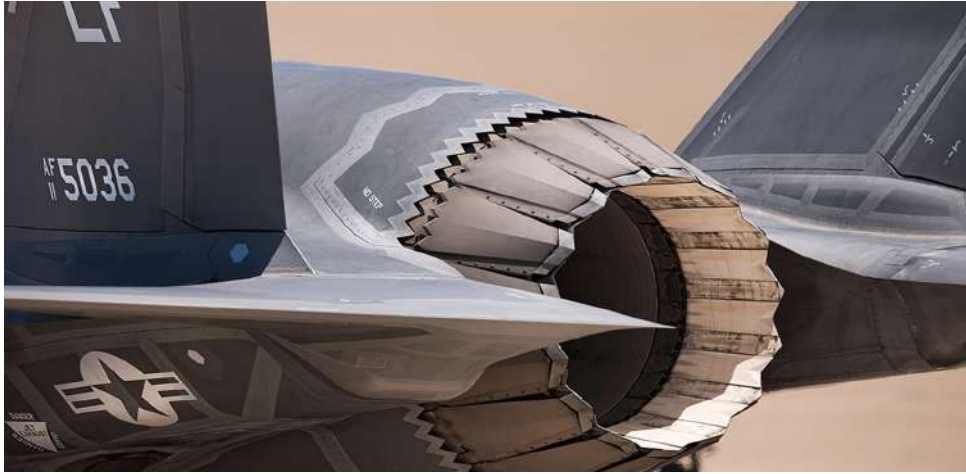
Figure 13: *The F-135 Low Observable Axisymmetric Nozzle [17]*

This configuration significantly reduced radar cross-section and infrared signature emissions from the engine. Maintenance costs were lowered as well.

Radar testing evaluate the unique shape and special coatings of the PW LOAN. The configuration achieved stealth through a combination of technologies, including geometric shaping, advanced cooling, temperature control and special coatings on internal and external surfaces. This exhaust system uses a cooled turbine face blocker, which allowed the engineers to avoid the use of a more impacting technique, i.e. serpentine exhaust duct. It also features a cooled nozzle to reduce in a significant way the aft sector infrared signature [18].

The main characteristics of the engines studied in this chapter, which are EJ-200, F-100-PW-229, F-119-PW-100 and F-135-PW-100m are summarized in the next *Chart*.

Table 1: *A comparison between different Engines studied in this chapter [2],[6],[10],[15]*

Engine/Parameter	EJ-200	F-100-PW-229	F-119-PW-100	F-135-PW-100
Length	3.99m	4.85m	5.16m	5.59m
Diameter	0.74m inlet	1.18m max, 0.88m inlet	1.20m max	1.17m max, 1.09m inlet
Dry weight	997kg	1735kg	1800kg	1701kg
Bypass Ratio	0.40	0.36	0.30	0.57
Maximum Dry Thrust	60kN	79.2kN	116kN	128kN
Maximum Wet Thrust	89kN	129.7kN	156kN	191kN
Wet Thrust to Weight Ratio	9.17	8.0	9.0	11.47
Fan System	3 stage	3 stage	3 stage	3 stage
High-Pressure Compressor	5 stage	10 stage	6 stage	6 stage
High-Pressure Turbine	1 stage	1 stage	1 stage	1 stage
Low-Pressure Turbine	1 stage	1 stage	1 Counter-Rotating Stage	2 stage
Nozzle	Convergent-Divergent	Convergent-Divergent	2D Vectoring Convergent-Divergent	Low Observable Axisymmetric Nozzle
Maximum Cruise Speed	2125km/h on Eurofighter	3087km/h on F-15, 2164km/h on F-16	3635km/h on F-22	1932km/h on F-35A
Turbine Inlet Temperature	1800K	1620K	1922K	2260K

2 Adaptive Cycle Engine: Origin and Technology

Rapid development in the early to mid 20th century led to aircraft propulsion moving from piston-powered propellers to turbojets and finally to turbofans. However, more time has now passed between the introduction of the low Bypass-Ratio Mixed Flow TurboFan in the 1950s and present day (circa 60+ years) than between the Wright Brothers first flight in 1903 to the introduction of the low BPR MFTF (about 50 years).

A first-pass examination of military aircraft over the last 60+ years might lead one to believe that there has been little effort to overcome the challenges posed by the turbojet and turbofan cycles.

Architecturally, the most modern military propulsion systems are essentially the same as those used 60 years ago. This is not to say that engine technology has not progressed. Advancements in materials and manufacturing, notably high-temperature resistant nickel super-alloys and single-crystal casting of turbine blades, has allowed the efficiency of engines to improve over time. However, the fundamental architecture has not changed since the 1950s.

2.1 The mission defines the cycle

Finding an engine cycle that operates optimally in all aspects of a mixed mission is impossible. Traditionally, it has been a question of choosing a best compromise, where the cycle parameters have been selected carefully to satisfy the most important performance aspects of the mission [19].

It is a trade-off between good supersonic performance (turbojet property) and low fuel consumption (possible with turbofans). The most obvious way to avoid this trade-off is to switch between the ideal engine cycle, i.e. to operate at the most optimal cycle at each mission phase. The afterburner implements the same idea. Instead of having separate engine components, where each is brought into use by directing flows (and thereby leaving temporarily the other components as dead mass), variable components can be used and be shared by different cycles. The latter principle promises optimum performance at low weight.

The purpose of engine selection is to provide an aircraft with enough thrust to fulfil a prescribed flight mission in all its elements, and do it with minimum fuel usage.

Regarding the engine, the thrust that can be extracted per captured airflow (Specific Thrust) needs to be high for good performance, and at the same time, the fuel flow relative to this thrust (Specific Fuel Consumption) needs to be low for the fuel economy. These properties are influenced by a number of engine parameters, such as compressor, fan and turbine pressure ratios, and combustion temperatures (in the core engine and the afterburner). Establishing an optimum set of all these parameters for a specific aircraft, satisfying its mission requirements, is the purpose of the engine design process.

In *Figure 14* we can see a mixed combat mission. It is clear that, in different segments, the engine is required to perform with very different main purposes, which we can resume in the two most important: lowering the Specific Fuel Consumption or giving maximum Specific Thrust.
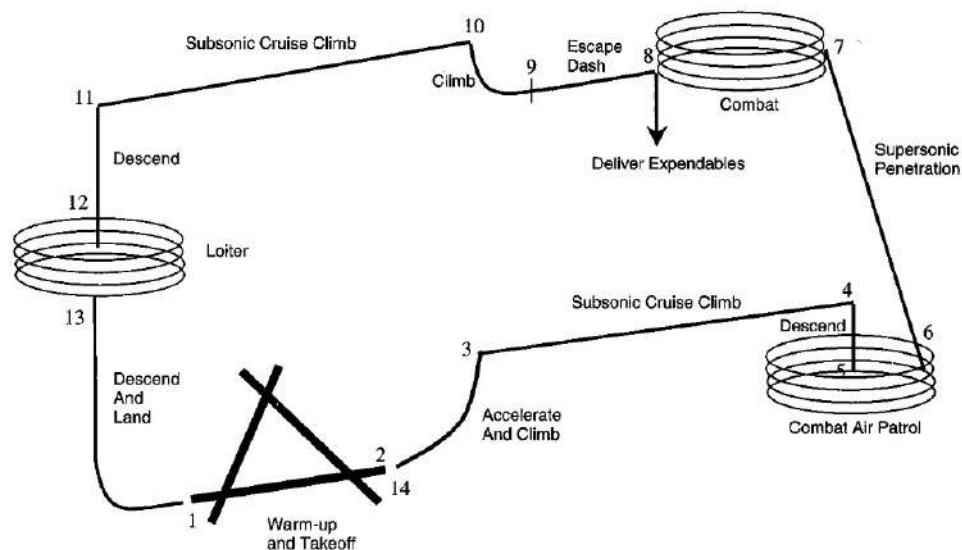

Figure 14: *An example of mixed mission profile divided by phases [19]*

By using Variable Cycle Engine, we can switch between different cycles depending on the mission segment we are in. It is like having multiple engine on board, although no parts are at idle in any moment (reduction in weight and size).

2.2 Comparison between a Variable Cycle Engine model and a fixed geometry Turbofan
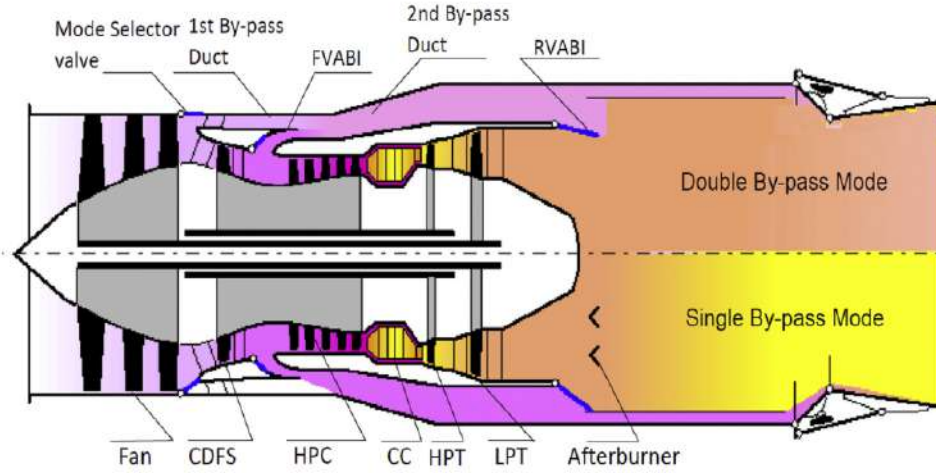

Figure 15: *The schematic illustration of a general VCE [20]*

The VCE model that we can see in *Figure 15* incorporates several main components such as Fan, Core Driven Fan Stage (CDFS), an additional fan stage driven directly by the engine's Core, rather than by the Low-Pressure Spool, High-Pressure Compressor (HPC), Combustion Chamber (CC), High-Pressure Turbine (HPT), Low-Pressure turbine (LPT), AfterBurner (AB) and Exhaust Nozzle (EN). This engine has also three variable geometries, i.e. a Mode Selection Valve (MSV), Front VAriable Bypass Injector (FVABI) and Rear VAriable Bypass Injector (RVABI) to direct the flow due to various requirements [20].

While upper side represents Double Bypass Mode (DBM), down side expresses Single-Bypass Mode (SBM).

To achieve the desired performance the geometry of engine components (RVABI and FVABI) are changed, and the MSV is adjusted.

The DBM is selected when the operation conditions are under subsonic cruise and the Specific Thrust (ST) needed is low, while the main objective is to achieve the maximum possible Specific Fuel Consumption (SFC). Total bypass ratio is 1.8. To meet this mode requirements, MSV, RVABI and FVABI are opened. Angle of Fan Guide Vane increases while angle of CDFS and HPC Vanes decrease in order to increase total by-pass ratio.

At SBM, when more ST is required, the total bypass ratio is 0.3. Angle of the Fan Guide Vane alternates to have the ability to match the inlet flow of the aircraft. In order to produce high specific thrust without critical performance losses, MSV is fully closed and RVABI is slightly closed. Most of the air passes through the CDFS and HPC components.

In this section we will compare a fixed cycle Low Bypass Turbofan at design point with our ACE model. For these two engines, we chose the following main parameters:

Table 2: *The parameters for ACE and Fixed Cycle Engine [20]*

Parameter	$\dot{m}_a$ [kg/s]	MSV	BPR_{tot}	T_{t4} [K]	T_{t7} [K]	π_{Fan}	π_{CDFS}	π_{HPC}	π_{tot}
Fixed Cycle low Bypass Turbofan									
Dry	101.69	-	0.67	1850	-	4.03	-	7	28.21
Wet	101.69	-	0.67	1850	2050	4.03	-	7	28.21
ACE model									
DBM	101.69	Open	1.8	1850	-	3.1	1.3	7	28.21
SBM	101.69	Closed	0.3	1850	2050	3.1	1.3	7	28.21

2.2.1 Specific Fuel Consumption, Specific Thrust and Efficiency comparison

Figure 16 presents SFC values regarding the fixed cycle turbofan and the ACE model for DBM and SBM.
Even though in a fixed cycle engine there are not different modes, we consider that DBM and SBM correspond to dry condition and wet condition, respectively for the fixed cycle turbofan.
As we can see the bypass change in the ACE clearly leads to decrease in the SFC value from 21.58 g/(kNs) to 17.85 g/(kNs) at DBM and from 50.69 g/(kNs) to 42.18 g/(kNs) at SBM.
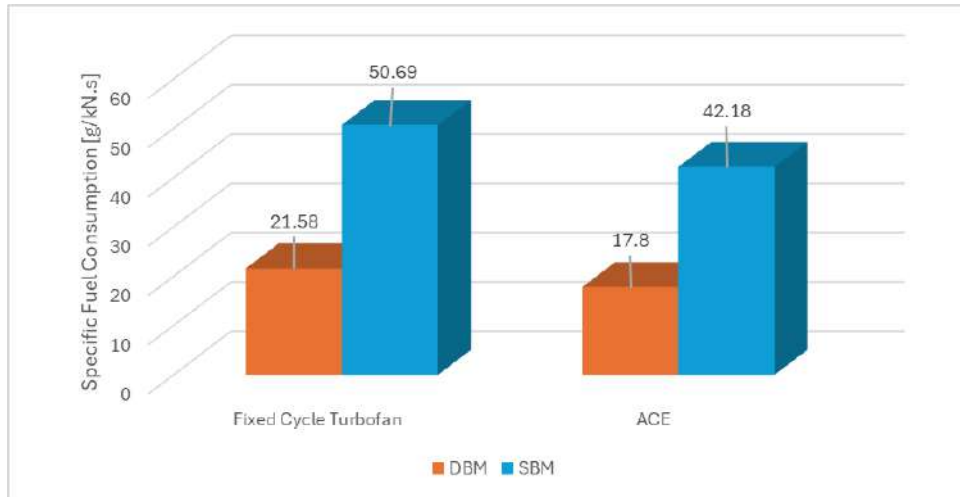

Figure 16: *The Specific Fuel Consumption of different engines for DBM and SBM [20]*

Figure 17 illustrates ST values of the two analyzed engine models. It's established that there is trade-off between engine parameters. For example, the decrease in ST can lead to experience performance loss.
Compared with fixed cycle turbofan, ST of the ACE model decreases with 23.86% at DBM. However, the ACE can compensate this performance loss by lowering by-pass ratio when required. On the other hand, ST value is slightly larger to fixed cycle's at SBM. From this improvement we can observe that components of the ACE work in compliance with each other well, i.e. the ACE model can reply requirements of both modes by changing running modes.
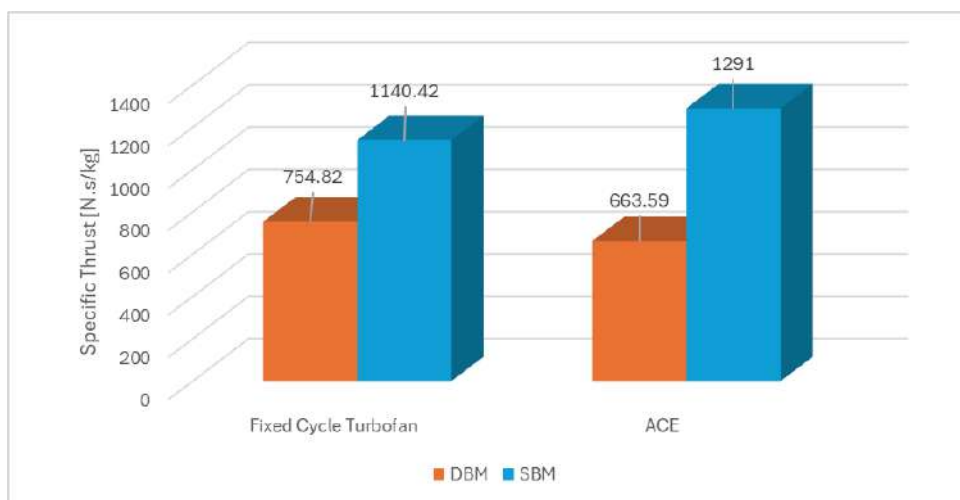

Figure 17: *The Specific Thrust of different engines for DBM and SBM [20]*

15

Another interesting comparison parameter is efficiency values. We calculated three different types of efficiency:

- Propulsion efficiency: ratio of thrust power to total power (wasted power plus thrust power).

- Thermal efficiency: ratio of total power to fuel power.

- Overall efficiency: multiplication of propulsion and thermal efficiencies.

Efficiency of the ACE and fixed cycle turbofan was computed by considering wasted and thrust powers in the study. From *Figure 18* the ACE model has higher efficiency at both two modes. When compared fixed cycle turbofan, propulsive, thermal and overall efficiencies of the ACE were determined as higher with 4%,6% and 5% respectively at DBM.
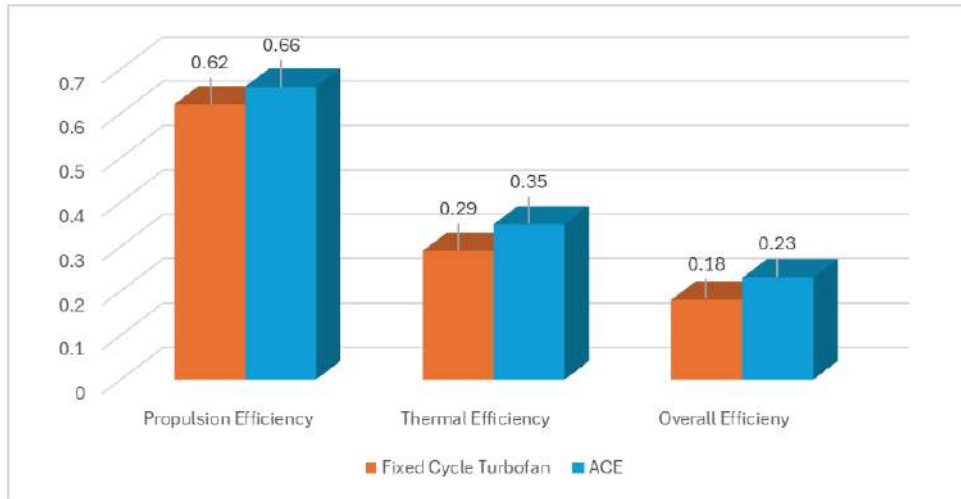

Figure 18: *The Efficiency values of different engines for DBM [20]*

Moreover, *Figure 19* presents that difference for these efficiencies is calculated in favour of the ACE with 5% for propulsive, 2% for thermal and 2% for overall at SBM.

Considering operating point from DBM to SBM, overall efficiency of the ACE model decreases from 23% to 9% whereas thrust efficiency of the ACE model reduces from 66% to 49%.
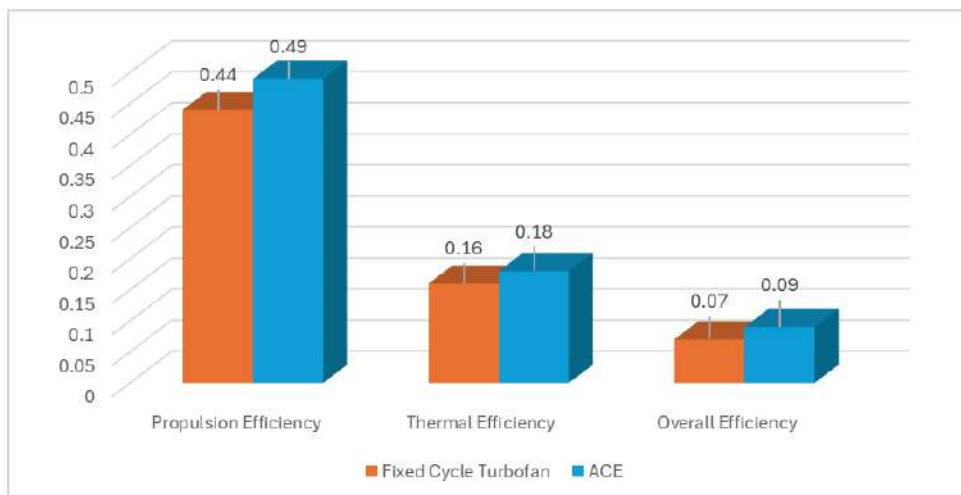

Figure 19: *Th Efficiency values of different engines for SBM [20]*

These results could be acceptable since thrust efficiency is inversely proportion with exhaust velocity.

One of air-breathing engines is to recover or decrease wasted power. If aircraft engines continuously run at high power, wasted power would increase depending on it.

Fixed cycle turbofan has fixed by-pass ratio. Even if high-thrust is not required, this type of engine continues generating relatively high power at lower engine operating point. High power means exhaust gases with high velocity.

Inlet air velocity is determined as 160 m/s for both two engines. For the ACE model, velocity of exhaust gases is computed as 475 m/s at DBM and 795 m/s at SBM, respectively. For the fixed cycle turbofan, exhaust velocity is registered at 550 m/s at Dry condition and 805 m/s at Wet condition.

2.2.2 Influence of different parameters on performance of an ACE for optimization

From now on we will only evaluate the performance of the ACE model, taking advantage of the possibility to change different parameters and optimizing this model.

The purpose is to determine how efficiency and wasted power are affected by a change in BPR .

BPR increment, ranging from 1 to 1.8 in DBM, increases overall efficiency and decreases wasted power. The increment in BPR leads to increase overall efficiency with 3.1%. However, wasted power decreases from 6.45 MW to 4.9 MW. If bypass ratio could not be increased, more energy than 1.55 MW is wasted through exhaust. The increase in BPR is desired until turbine work meets required power for Fan, CDFS and HPC.
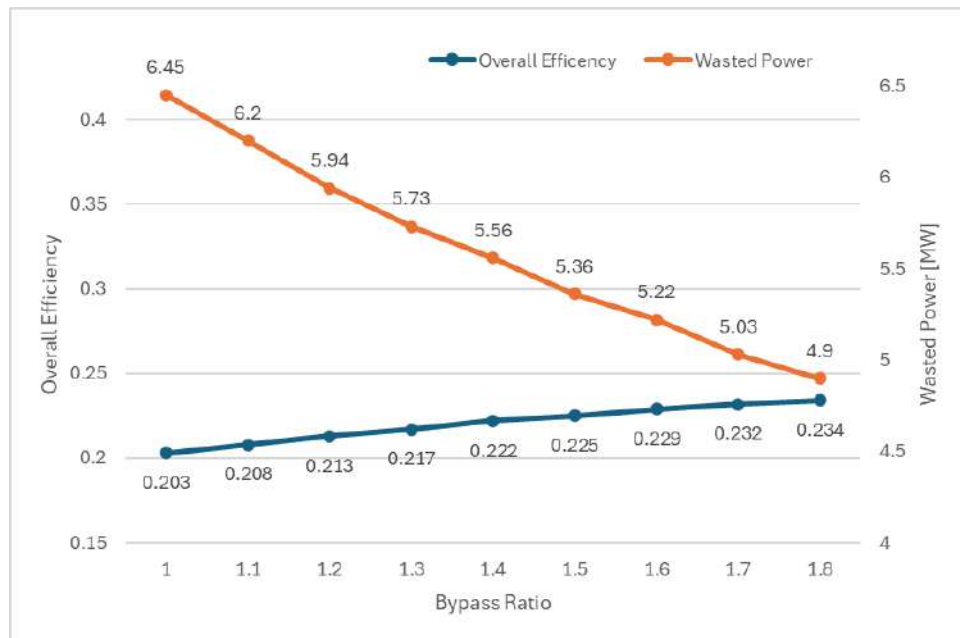

Figure 20: *The effects of Bypass Ratio on Overall Efficiency and Wasted Power value for DBM* [20]

Effect of turbine inlet temperature (T_{t4}) on these parameters are presented in *Figure 21*. Its increase affects favourably overall efficiency, but adversely wasted power in terms of the engine performance at DBM. T_{t4} increases exhaust velocity, so both wasted power and thrust power increase. The improvement in overall efficiency occurs with 4.1%. However, wasted power increases from 4.22 MW to 5.09 MW at DBM.

The increase in T_{t4} is desired up to a point that turbine materials can withstand. We will discuss this topic later in this dissertation.
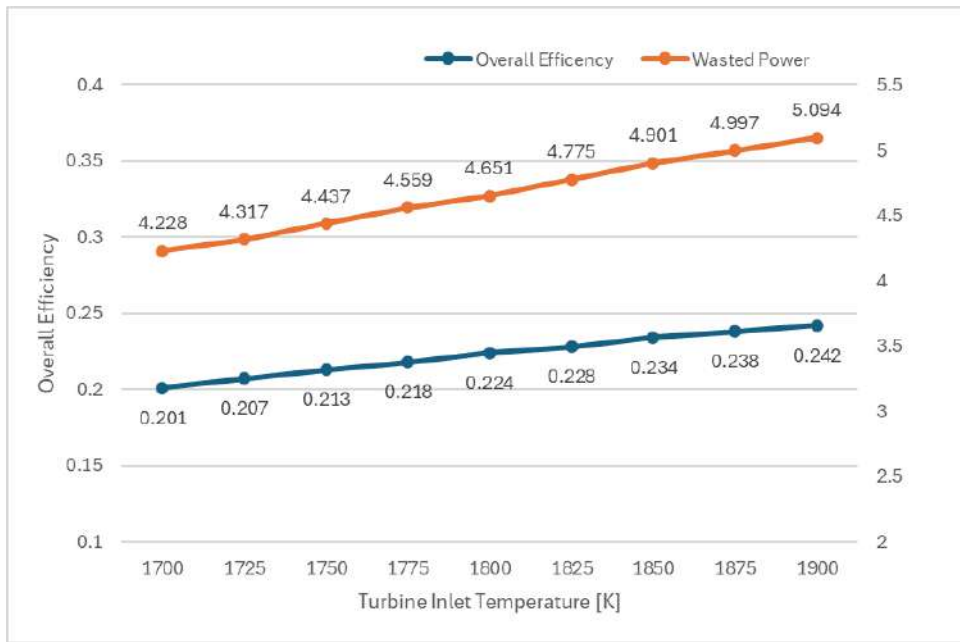
Figure 21: *The effects of T_{t4} on Overall Efficiency and Wasted Power value at DBM* [20]

Effect of Bypass Ratio on ST and SFC for the both modes is evaluated.

BPR of the ACE model is modulated, ranging from 0.3 to 1.8. The reason why BPR can not exceed 1.8 is that turbine components can not satisfy required power to Fan, CDFS and HPC components.

For these analysis T_{t4} of 1800K and a π_{HPC} of 7 were chosen.

The increase in Bypass Ratio decreases SFC value from 20.15 g/(kNs) to 17.85 g/(kNs) at DBM. This decrease corresponds to a 11.4%. Since less air mass flow is accelerated in the core engine while increasing the BPR, ST value decreases from 845.3 (Ns)/kg to 678.4 (Ns)/kg at DBM, with a 19.7%.
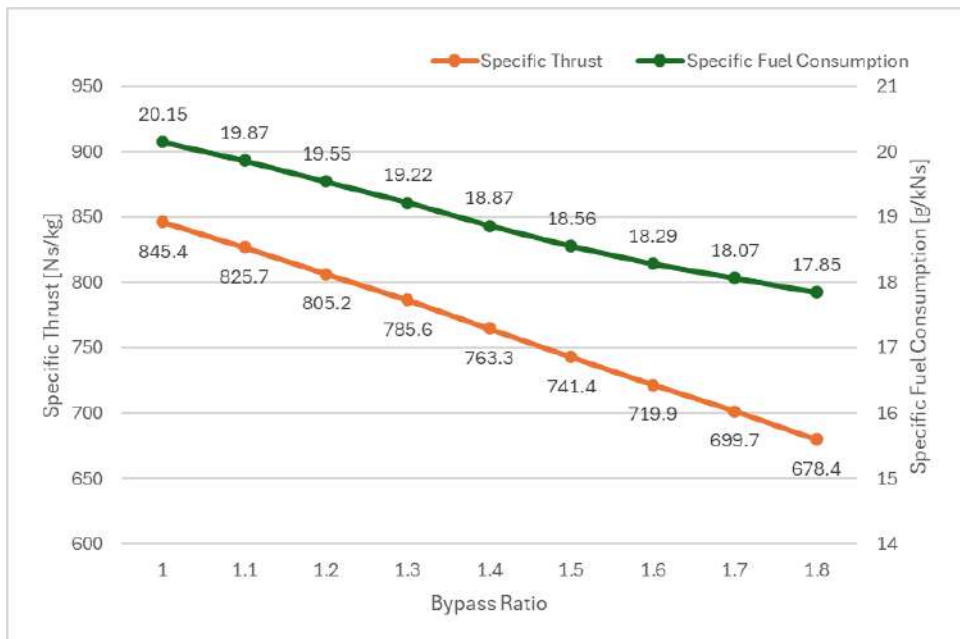

Figure 22: *The effects of BPR on SFC and ST values at DBM* [20]

18

As for SBM, the increase in BPR is not a desired condition because BPR increases SFC value from 42.18 g/(kNs) to 48.03 g/(kNs). Moreover, ST value decreases with the increase of BPR. In this mode, BPR is desired as low as possible in terms of performance parameters. Therefore, the ACE model works as a turbojet cycle in the SBM. When BPR increases, the ST value decreases with ratio of 12.19% at SBM.
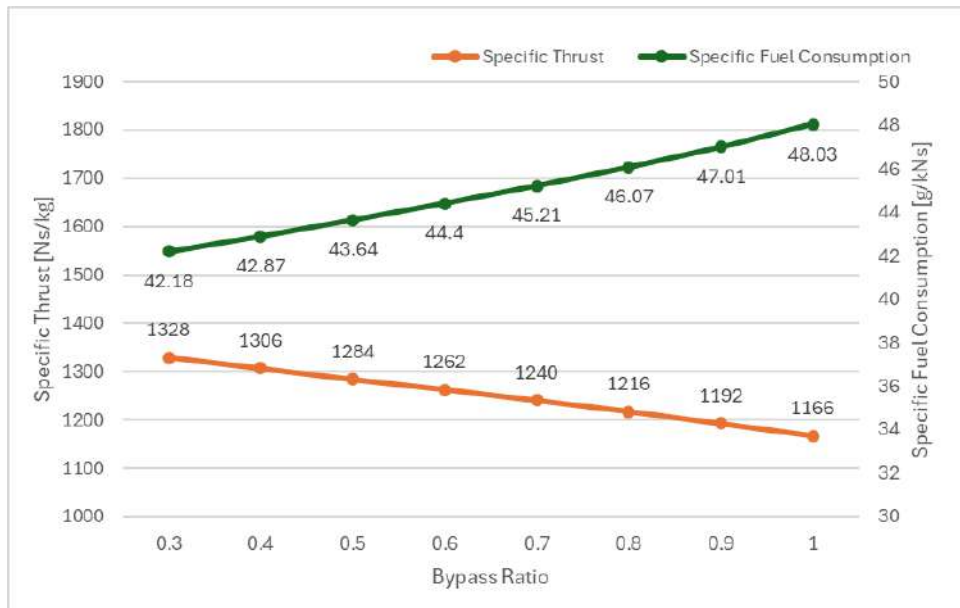
Figure 23: *The effects of BPR on SFC and ST values at SBM [20]*

We now analyze the effects of other two design parameters: π_{HPC} and T_{t4}.

For what concerns the first one, we have to fix BPR value at 1.8 at DBM and 0.3 at SBM. In addition, T_{t4} is 1800K for both modes. The increase of this parameter enhances performance of the ACE model at DBM. Namely, SFC changes from 18.23 g/(kNs) to 17.53 g/(kNs). The SFC decrease corresponds ratio of 3.83% at DBM. A trade-off analysis between the design parameters and performance parameters are necessary, so design variables do not have same effect on performance characteristics for all modes.

Likewise, the increase in T_{t4} has different effects on SFC at SBM. As for SBM, SFC is adversely affected by increasing pressure ratio of HPC. SFC changes from 41.72 g/(kNs) to 42.81 g/(kNs) Namely, SFC increases with ratio of 2.63%.
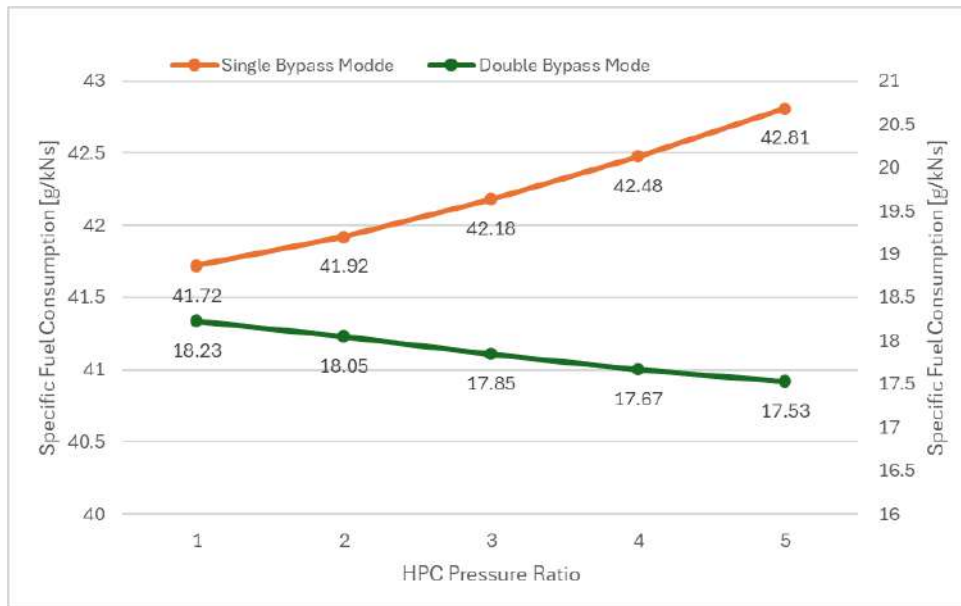
Figure 24: *The effects of HPC Pressure Ratio at DBM and SBM [20]*

To analyze the effects that Turbine Inlet Temperature has on SFC parameter at DBM and SBM, we need to fix π_{HPC} at 7. BPR has also a fixed value of 1.8 at DBM and 0.3 at SBM, as it was before.

The increment of temperature affects favourably SFC value for both modes. As we can observe from the following chart, when comparing these two modes, effect of T_{t4} is higher at SBM. Namely, the increase in temperature decreases SFC value from 18.64 g/(kNs) to 17.66 g/(kNs) at DBM. The decrease is calculated as 5.25%.

Moreover, SFC value decreases from 45.73 g/(kNs) to 41.35 g/(kNs) with the increase of T_{t4} at SBM. The decrease corresponds 9.57%.

Figure 25: *The effects of Turbine Inlet Temperature on SFC ad DNM and SBM [20]*

Investigating these various effects of design parameters help in optimizing effectively performance parameters because each design parameter affects performance parameters with different intensity.

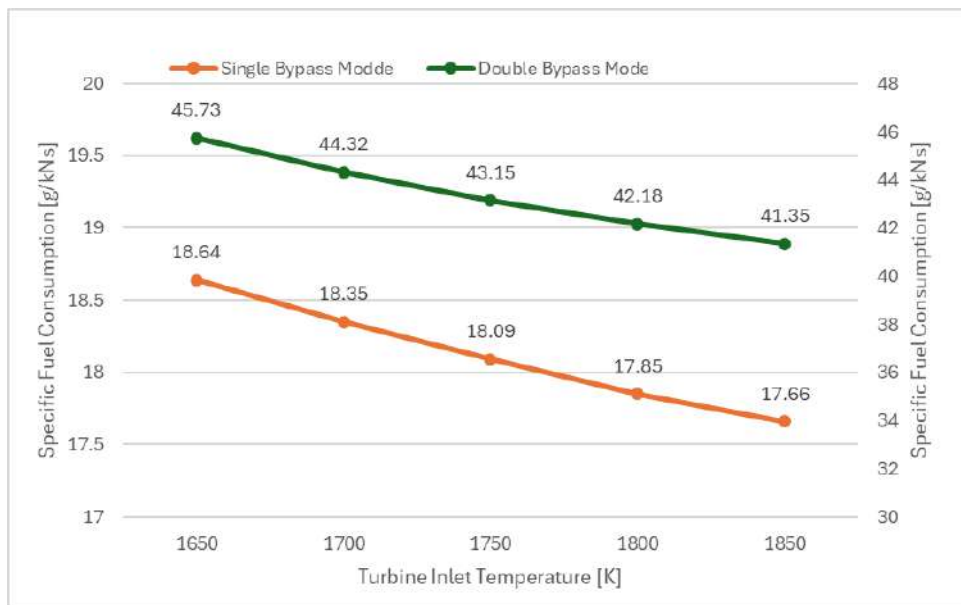The following figures present High-Pressure Compressor mappings at DBM and SBM. These can ensure that HPC can stably works for selected operating points.

These mappings incorporate surge line, efficiency line and speed line. As can be understood that corrected HPC mass flow, which is determined with relative temperature ratio and pressure ratio, changes with Bypass Ratio and working modes. The efficiency contours for HPC show adiabatic efficiency, varying between 0.85 and 0.86. Operating ranges are also showed in the pictures. As can be seen, HPC PR can change between 6 and 8 without surge event.
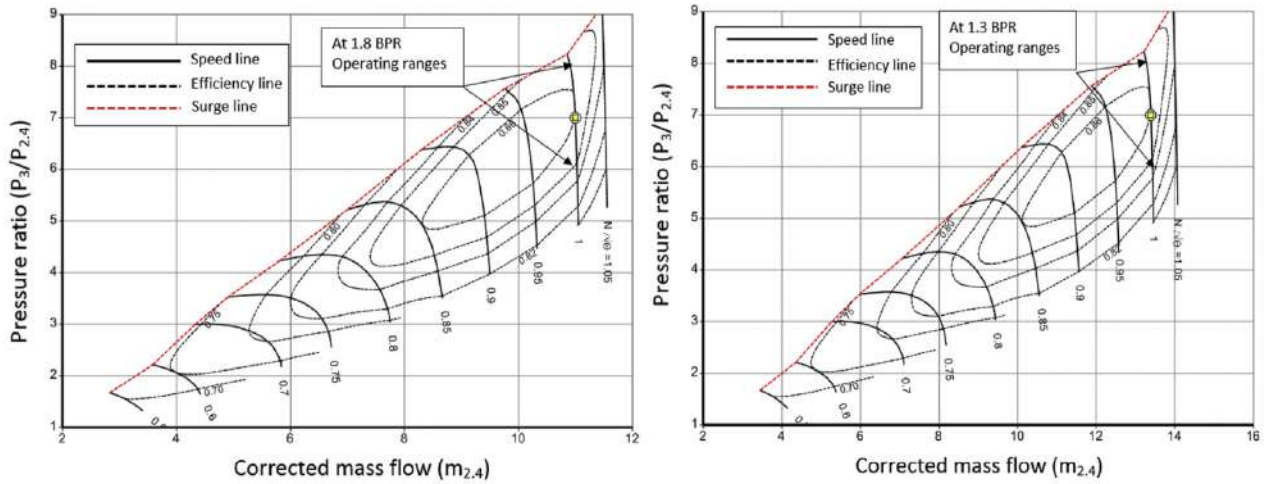
Figure 26: *The HPC mapping for 1.3 and 1.8 of BPR at DBM [20]*
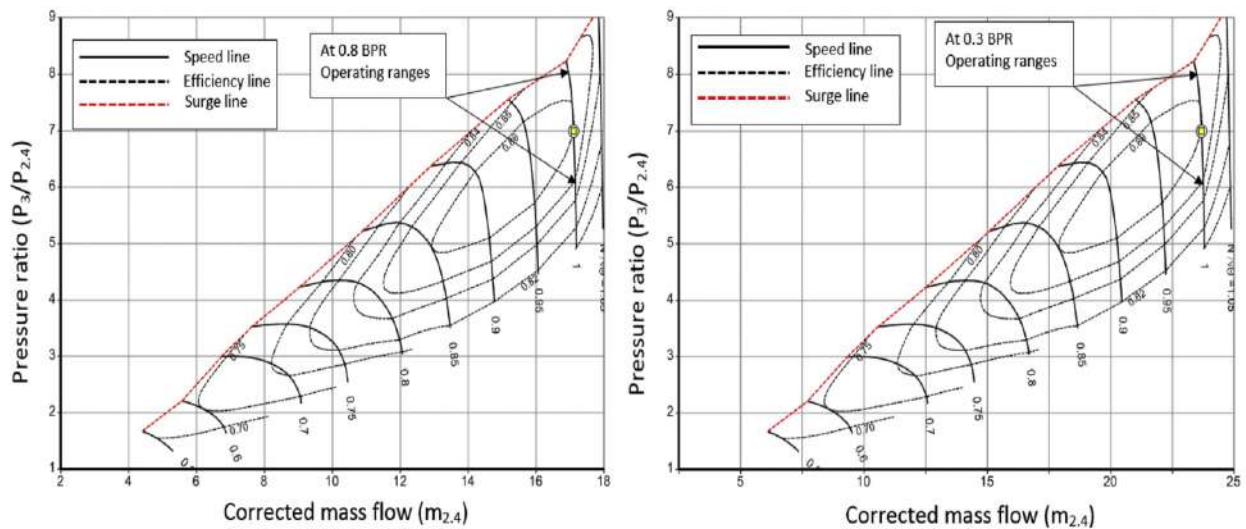
Figure 27: *The HPC mapping for 0.8 and 0.3 of BPR at DBM [20]*

For the optimization process BPR, T_{t4} and π_{HPC} are chosen as design variables. Their ranges are respectively 1.3<BPR<1.9 for DBM and 0.3<BPR<0.8 for SBM. For the temperature the range was chosen between 1650K and 1850K, and for the π_{HPC} the value was between 6 and 8.

According to optimization results minimum SFC value of the ACE model at DBM are determined as 17.65 g/(kNs). BPR, T_{t4} and π_{HPC} values which correspond to this result are 1.8, 1850K and 7.65 respectively. Before optimization results,

SFC value was calculated as 17.85 g/(kNs) with 1.8 of BPR value, 1800K of T_{t4} value and 7 of HPC pressure ratio. In terms of SFC, the obtained benefit through optimization tool is computed as 2.71% at DBM.

As for SBM, minimum SFC value is calculated as 40.60 g/(kNs) at SBM. For this aim, BPR and T_{t4} values are determined to be 0.3 and 1850 K respectively, while π_{HPC} value was found at 6.5. Considering initial value of SFC, the optimization process provides the less SFC value with 1.77%.

2.3 Evolution of VCE: the Adaptive Cycle Engine

The Adaptive Cycle Engine is developed from the Variable Cycle Engine with the latter surrounded by an additional bypass stream in order to improve spillage drag at off-design points.

In cruise mode more air will flow through the third stream resulting in the high bypass engine giving lower fuel consumption. On the other hand, the engine will function as a low bypass turbofan engine giving more thrust by allowing more air to flow through core while in combat.

This engine changes the bypass ratio and the fan pressure ratio, which are the main parameters affecting fuel consumption value of the engine and thrust values.
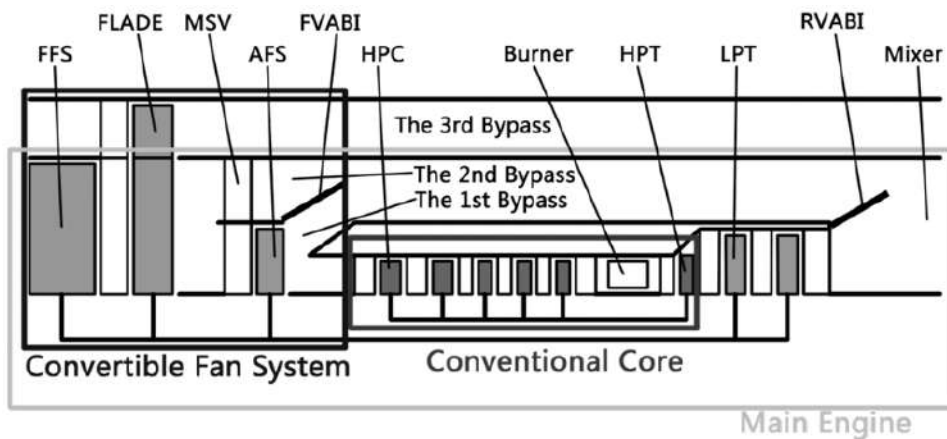

Figure 28: *The schematic model of ACE [21]*

The baseline ACE shown in *Figure 28* is made up by a Front Fan Stage (FFS), a Fan on Blade (FLADE) and an Aft Fan Sage (AFS). Since these are variable area structures which can be actively adjusted to modify the engine BPR and PR distribution, we can refer to these components as Convertible Fan System (CFS).

The CFS divides engine flow path into three bypass flow paths and one inner flow path. According to the order from the inside to the outside, we can refer to these three bypass as 1st, 2nd and 3rd.

The Mode Selection Valve, as we have seen in the VCE, is located upstream the second bypass. It is driven by a pressure gradient and it has only two states (open and closed) to control whether the air flow from FFS could flow into the second bypass or not.

FLADE guide vane is another essential component of the ACE. This could be adjusted to different angle, changing the air flow rate through the third bypass more flexibly. Especially, while FLADE guide vane is adjusted to a very small angle (-85°), there is little air flow through the third bypass and FLADE would hardly compress the air flow. Therefore, while FLADE guide vane is at the angle of -85°, the 3rd bypass could be approximately considered as closed. While FLADE guide vane is at the other angles, the third bypass could be considered as open.

The effect of FLADE on SFC and ST is very similar to the one discussed for the inner bypass. Increasing Bypass Ratio will decrease Specific Thrust and reduce Specific Fuel consumption for all three bypass streams.

2.3.1 Comparison between F-119 and an ACE model

To better understand the benefits brought by ACE, the latter was compared with the GE F-119, the engine of the F-22 Raptor [22]. This comparison was executed at two different off-design point:

- Transonic Cruise at 35,000 ft and Mach 0.8

- Supersonic "Combat" at 40,000 ft and Mach 2.2

22

For these off-design points, there had been selected two different on-design point configurations shown in *Table* for the ACE.

Table 3: *The parameters for the chosen on-design point* [22]

Parameter	1st & 2nd BPR	3rd BPR	$\pi_{1st\ Fan}$	$\pi_{2nd\ Fan}$	π_{HPC}	LP Shaft [RPM]	HP Shaft [RPM]	T_{t4} [K]
Subsonic Cruise	0.391	1.330	3.410	1.907	5.961	4872	9409	2000
Supersonic Combat	0.378	1.679	1.959	1.665	4.824	4185	10753	2222

Once the design configurations were selected, best possible combination for Inner Bypass Ratio and $\pi_{2nd\ Fan}$ for each off-design point were studied and obtained.

Table 4: *The engine working parameters at different off-design point* [22]

Parameter	1st & 2nd BPR	$\pi_{2nd\ Fan}$
Subsonic Cruise	1.2	1.4
Supersonic Combat	0	1.6

After the off-design performance were calculated, these were compared in *Table* and *Table* with the performance at the same off-design points for the F-119.

Table 5: *A comparison of our ACE model with the F-119 at Transonic Cruise* [22]

Parameter	2n fan	2nd Bypass Ratio
Subsonic Cruise	0.391	1.330
Supersonic Combat	0.378	1.679

Table 6: *A comparison of our ACE model and the F-119 at Supersonic Combat* [22]

Parameter	2n fan	2nd Bypass Ratio
Subsonic Cruise	0.391	1.330
Supersonic Combat	0.378	1.679

It can be observed that Adaptive Cycle Engine produces lower SFC values at all operating conditions when compared to the F-119.

It also produces more thrust than the F-119 in Combat conditions. The F-119 has comparable thrust to the adaptive cycle engine for Transonic cruise but has very large value of SFC when compared to the Adaptive Cycle Engine.

Changing the parameters in off-design conditions will result in a more complicated mechanical design, but will also have tremendous advantages in increasing thrust and decreasing fuel consumption, with an overall performance increase in gas turbine engine.

2.3.2 Benefits on subsonic climb

Another important condition of the flight envelop is subsonic climb. Although it occupies a relatively short time in the whole flight mission, the fighter's climbing performance is still one of the key factor determining the combat capability of fighters since the latter need the engine to provide enough thrust in order to shorten the climbing process time as much as possible.

On the other hand, because of its relatively short time, even if the fuel consumption is slightly higher, it still has relatively less impact on the combat radius of the fighter.

Therefore, engine thrust should be the only objective of the optimization process in this section.

For this optimization, the reference model of ACE is the one shown in *Figure 28* and the maximum High-Pressure Turbine Inlet Temperature is set at 2100K.

We can identify four different operating modes divided by the combinations of different states of both MSV and bypass.

When both MSV and the third bypass are closed, we define the operating mode as Mode 1. Engine in Mode 1 could produce greater Specific Thrust either with or without afterburner, and was demonstrated suitable for air combat.
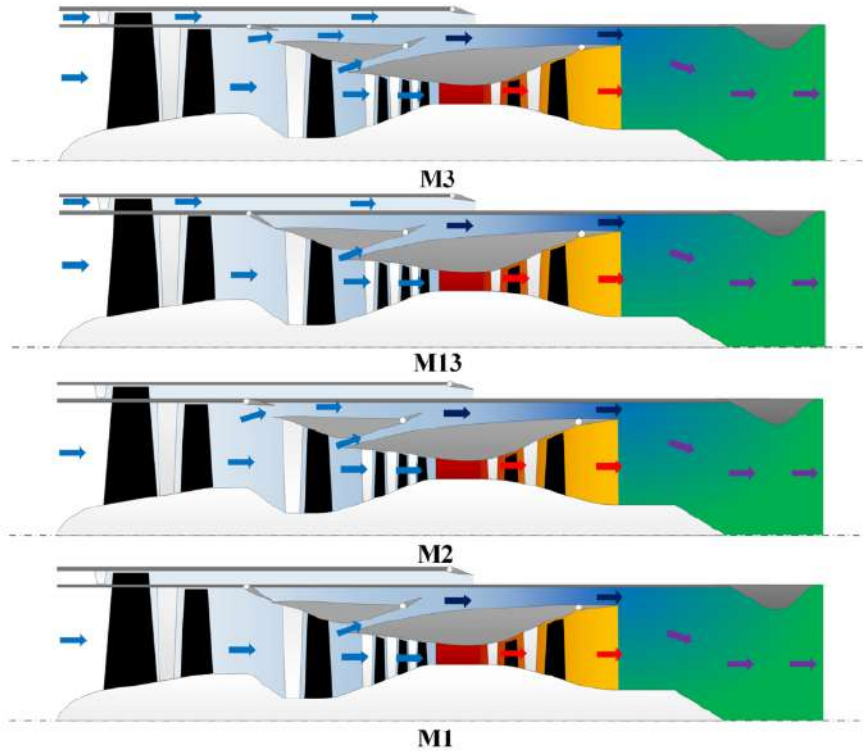
Figure 29: *The different working modes for an ACE model[34]*

While MSV is open but the third bypass is closed, the operating mode of engine is defined as Mode 2. Engine in Mode 2 produce more thrust while engine inlet temperature is high, because of its relatively lower turbine entry temperature.

While MSV is closed but the third bypass is open, the operating mode of engine is defined as Mode 13. Engine in Mode 13 would produce greater thrust without afterburner at subsonic and low supersonic flight conditions.

While both MSV and the third bypass are open, the operating mode of engine is defined as Mode 3. Engine in Mode 3 has relatively lower specific fuel consumption without afterburner owing to its higher overall bypass ratio, and is demonstrated suitable for cruise.

Engine Specific Fuel Consumption of Mode 1 and Mode 2 are higher than those of Mode 13 and Mode 3 at the altitude and Mach number range, respectively between 0 and 11km and 0 and 1.2 Mach.

It's mainly due to the open of the third bypass at both Mode 13 and Mode 3, which obviously increases the total bypass ratio. For the same reason as above, engine thrust of both Mode 13 and Mode 3 are obviously better than those of Mode 1 and Mode 2.

Moreover, because ACE working at Mode 13 has greater specific thrust, the engine at Mode 13 would produce greater thrust regarding both altitude and Mach number for subsonic climb.

As a result, Mode 13 is the most suitable operating mode for subsonic climb.

In the process of fighter climbing, the total temperature of the inlet is constantly changing. According to the adjustment schedule, the engine needs to constantly adjust the variable geometry mechanisms to maintain the optimized thrust.

However, it is difficult to realize in the actual climb process, because the continuous adjustments of those variable geometry mechanisms will make the engine work in the transition state for a long time, which is disadvantage of the engine's aerodynamic stability.

Therefore, in order to asses the influence variable geometry mechanism adjustment on climb results, if we compare the climbing performance, the performance of the optimized ACE, the performance of ACE without adjusting variable geometry mechanisms (ACE fixed) and the performance of the mixed-flow turbofan used as reference would be all used to calculate the climb results.

In order to have a more comprehensive comparison of the climbing performance, equal Mach number climb was selected. The starting point of equal-Mach number climb is set at altitude 0 km and Mach number 0.90, as well as the end point is at altitude 11km and Mach number 0.90. The initial weight of the fighter is slightly different to the full load state.

As illustrated before, ACE has notable advantages of both climbing time and fuel consumption. In details, the climbing time of the fixed ACE is 21.13% shorter than that of the conventional turbofan, and the optimized ACE shortens the

climbing time by 37.83%.
At the same time, the fuel consumption of the fixed ACE is 8.68% less than that of the conventional turbofan, as well as the fuel consumption of the optimized ACE is 11.24% less than that of the conventional one.
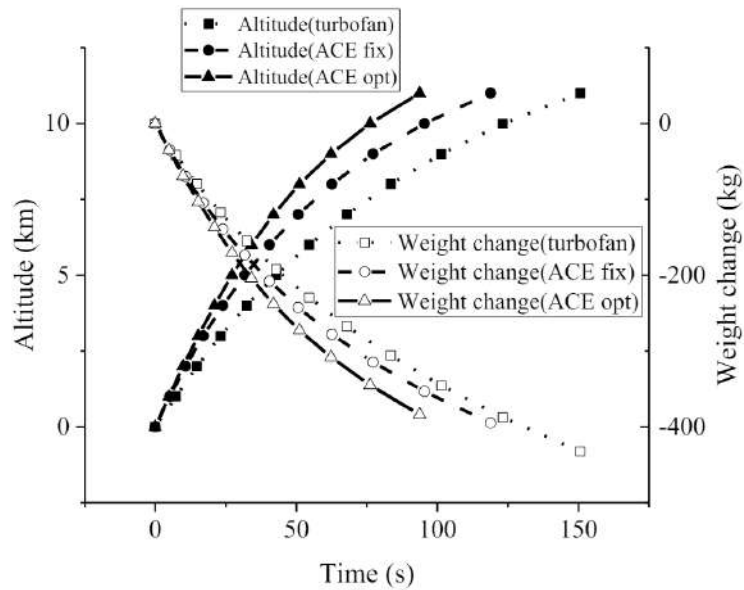

Figure 30: *A comparison between a conventional Turbofan, a fixed ACE and an optimized ACE at equal Mach number climb [21]*

ACE could produce greater climbing thrust using mode conversion.
Hence, fighter jets equipped with and ACE rather than a fixed cycle engine would take advantages of both climbing time and total fuel consumption.

2.4 A different idea for ACE: reduction of the variable geometries and its effects on constant airflow

The introduction of extensive variable geometries brings with it several benefits regarding the modulation's flexibility of thrust and airflow. However this process can increase the complexity of the engine's configuration, resulting in high technical risk.

For example, the nozzle area of the HPT guide vane is an important parameter, which affects the operating line of the compressor and the operational flexibility of the engine. However, the entry temperature of the HPT (T_{t4}) guide vane is extremely high, which makes it dangerous to install variable geometries. Therefore, a study is needed to understand the necessity of installing variable geometries into the HPT guide vane.

Moreover, the typical configuration of the ACE is a three-bypass engine, which is difficult to be derived from the existing gas turbine engines.

There are several components with innovative technologies. Therefore, before the further development of a three-stream ACE model, it is opportune to research the related control systems. Therefore, it is favorable to design an ACE with simpler configuration as the initial platform for the researches and tests of the components and control system at first.

Due to the motivations mentioned above, in this section the three-stream ACE shown in *Figure 31* is studied and compared with a traditional ACE model shown in *Figure 32*.
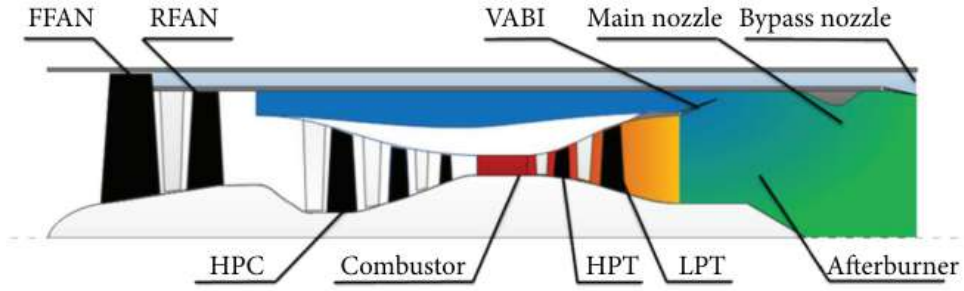
25

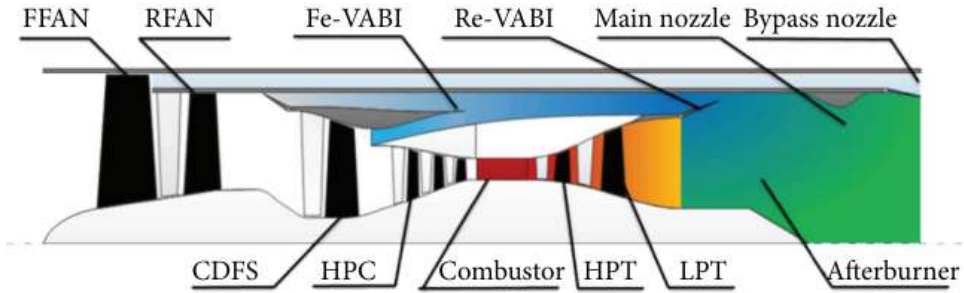Figure 31: *The schematic representation of a three stream ACE model [23]*

Figure 32: *The schematic representation of a three Bypass ACE model [23]*

The design point is at sea level static condition, and its parameters are shown in the following chart.

- $\mathbf{W_a}$: total airflow
- $\mathbf{D_F}$: diameter of the engine fan entry
- $\mathbf{B_{tot}}$: total bypass ratio
- $\mathbf{B_1}$: first bypass split ratio
- $\mathbf{B_2}$: second bypass split ratio

Table 7: *The working parameters at the design-point of a three stream ACE [23]*

Parameter	W_a [kg/s]	T_{t4} [K]	D_F [m]	B_{tot}	B_1	B_2	π_{tot}	π_{FAN}	π_{FFAN}	π_{RFAN}	π_{HPC}	N_1
Value	165	1750	1.052	1.0125	0.4375	0.4	32	3.404	1.84	1.85	9.30	100%

The initial number of variable geometries is seven. They are:

- Variable Stator Vane of RFAN (VSV$_{RFAN}$)
- Variable Stator Vane of HPC (VSV$_{HPC}$)
- Variable Area Nozzle of HPT Guide Vane (VAN$_{HPT}$)
- Variable Area Nozzle of LPT Guide Vane (VAN$_{LPT}$)
- Variable Area section of Main Nozzle's Throat (A_8)
- Variable Area section of Bypass Nozzle's Exit (A_{28})

After analyzing the effects of varying every above mentioned geometries, only five of them were selected as necessary. The selection scheme is determined through several combined control analyses. At first, only the variable geometries with greatest effects on the ACE thrust will be selected. Based on the analysis performed, the combined control schedule of these variable geometries can be designed to modulate thrust with constant airflow.
The variation range of the thrust will be limited by several constraints, such as components' surge margin and efficiency.

- **Group 1**: Firstly, considering A_8 and VSV_{RFAN} have an obvious effect on the thrust and an opposite effect on the airflow, they are selected as the first group to control the throttling process while others are kept unchanged. Through turning up A_8 and turning down VSV_{RFAN}, the airflow can be kept constant as the thrust reduces. The thrust decreases from 100% to 83.19% during subsonic cruise and to 82.53% during supersonic cruise with constant airflow. The result shows that η_{FFAN} limits the upper bound of the thrust and airflow limits the lower bound of the thrust. If A_8 and VSV_{RFAN} are adjusted to increase the thrust further, η_{FFAN} will drop beyond the lower bounds. If A_8 and VSV_{RFAN} are adjusted to decrease the thrust further, the airflow cannot be kept constant.

- **Group 2**: Therefore, additional variable geometries should be selected to broaden the variation range of thrust. A_{28} is selected as an addition to the first group due to its great effect on airflow and SM_{FFAN} (Surge Margin of the Front Fan). Through turning down A_8 and turning up VSV_{RFAN} further, the thrust rises but η_{FFAN} tends to drop beyond the lower bound. In that case, turning down A_{28} can improve η_{FFAN} and this broadens the variation range of the thrust with constant airflow. With the second group of variable geometries, the thrust decreases from 100% to 67.77% during subsonic cruise and to 65.2% during supersonic cruise with constant airflow. However, if the variable geometries are adjusted to modulate the thrust in a wider range, SM_{RFAN} and η_{RFAN} tend to drop beyond the lower bound.

- **Group 3**: VAN_{LPT} should be selected as the addition to third group of variable geometries considering its great effect on SM_{RFAN} and η_{RFAN}. However, VAN_{LPT} also has a great effect on η_{HPC} and SM_{HPC}, which is different from the other variable geometries in the second group. In order to fulfill the potential of VAN_{LPT}, VSV_{HPC} is also selected. Through the combined control of variable geometries in group 3, the thrust decreases from 100% to 60.36% during subsonic cruise and to 59.81% during supersonic cruise with constant airflow.

Control schedule of group 3 variable geometries is shown in the following table.

Table 8: *The control schedule of variable geometries [23]*

Parameter	Thrust Reduction	VSV_{RFAN}	VSV_{HPC}	VAN_{HPT}	VAN_{LPT}	VABI	A_8	A_{28}
Subsonic	100%	0°	0°	1.0	1.1	1.0	0.95	0.8
	60.36%	-30°	-20°	1.0	0.92	1.0	1.1	1.2
Supersonic	100%	0°	0°	1.0	1.1	1.0	0.95	0.8
	59.81%	-30°	-20°	1.0	0.95	1.0	1.08	1.15

Since VABI didn't have great effects on thrust and airflow compared to the other geometries it is unnecessary to introduce variable geometries into it.

Moreover, since VAN_{HPT} operates at extremely high temperature and needs a complex cooling system to maintain its safety and durability we managed to reduce thrust maintaining constant airflow without introducing VAN_{HPT} as a variable geometry.

We compared the results obtained from the three stream ACE with the one from three bypass stream ACE in *Table*.

Table 9: *Thrust reduction comparison between a three stream ACE and a three bypass ACE [23]*

	Three stream ACE	Three Bypass ACE
Subsonic	60.36%	45.10%
Supersonic	59.81%	68.31%

During subsonic throttling, three bypass ACE operates at double bypass mode with a lower bypass ratio at first. Then, it transforms to triple bypass mode with a higher bypass ratio in order to make thrust to reduce more. With double operating modes, three bypass ACE can change the uninstalled thrust in a wider range during the subsonic throttling.

However, the three bypass ACE can only operate at double bypass mode during the supersonic throttling phase. Therefore, if we compare it with the three stream ACE, the three bypass ACE has a narrower variation range of uninstalled thrust during supersonic throttling.

In summary, the three-stream ACE is a trade-off design between the technical risk and the variable cycle characteristic. The improvement of the three stream ACE installed performance is not as high as the three-bypass ACE's, but it is less complicated and is easier to be designed. If we consider the technical feasibility, three stream ACE is a better platform regarding costs and risks. With the future technical progress in component and control system, the three-bypass ACE and other complex types of ACE will be the better choices to achieve more improvement of installed performance and other variable cycle characteristics.

3 Adaptive Cycle Engine: Feasibility and Further Development

From the first propose of Adaptive Cycle Engine concept, several different configurations of Adaptive Cycle Engine concepts had been proposed, studied and demonstrated. However, it is still a problem to identify the different features of each configuration of Adaptive Cycle Engine and the differences between each other.

Many different new ideas are being developed and with the advancement in technology new variable geometries have been introduced in new pioneering ACE models.

One example is the Core Driven Fan Stage [24], a component that lies between the Mode Selection Valve and splitter of the first bypass. Since its design is very complicated, it can be replaced by a simpler Fan driven by the Low-Pressure Turbine.

An even more sophisticated element is the Core FLADE [25] which substitute the CDFS. It is a diverter ring between the first bypass and the core engine, and the airflow is separated by a splitter before it enters the first bypass and the core engine, with a similare shape to the FLADE.

These and many others innovative variable geometries, are being studied. At this time, the implementation of these elements seems to bring little benefits (very small advantages in performance and slightly better for what concerns matching between components) and many problems regarding difficulties in design, reliability and costs, always increasing the weight of the engines.

3.1 Multi-Point Design

To successfully optimize the performance of a supersonic aircraft, its mission profile, thermal systems, and engine design need to be considered simultaneously. To do so we need to construct a complex interconnected model that can be used in a gradient-based optimization problem [26].

Conventionally, an engine is designed at a single operating point, frequently this point is the sea-level static (SLS) condition. Nevertheless, we are interested in the engine's performance at other flight conditions as well.

We can vary the fuel flow through the engine to control the thrust, and then solve for the shaft speeds to ensure the engine performance can be calculated correctly. The mass flow rates, net power output, pressure ratios, rotational speeds of the shafts, flows for each compressor, and turbine pair must match.

To solve these matching equations, the initial guesses inputted into the model are extremely important. Without good initial guesses the model does not converge successfully. The model was converged at different flight conditions and saved these results. Using this data, a surrogate model that provides good initial guesses has been created for the engine model at any given flight condition, even when changing the engine's static design. The Mach-altitude points for this surrogate are shown in *Figure 33* to illustrate the tested flight envelop.
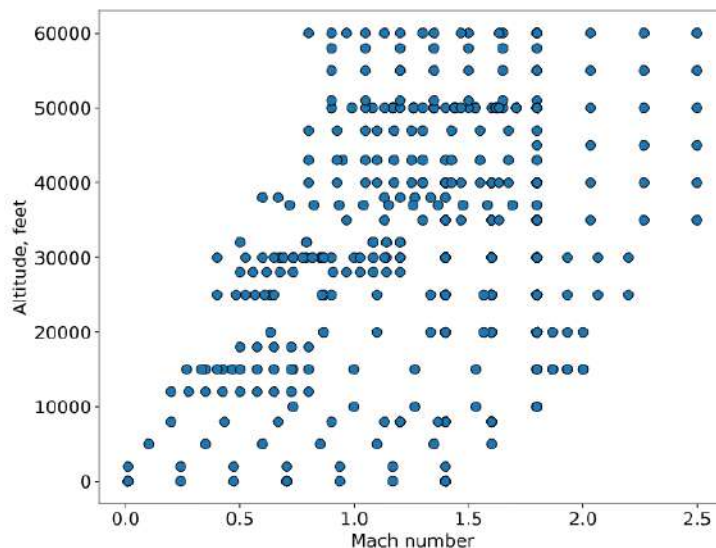

Figure 33: *The Mach-altitude flight envelop[26]*

To perform the optimization design, five different parameters have been selected.

- π_{tot}: total pressure ratio of both compressor stages

- π_{fan}: pressure ratio of the fan

- π_{bp}: ratio of the pressure levels in the bypass to the core exhaust ducts

- $F_{\text{net,SLS}}$: desired thrust of the engine at the design point, which requires a certain mass flow rate

- **FAR**: fuel-to-air ratio. It influences how much fuel is added into the burner, which is the main driver for thrust production. Although FAR is a design variable, it is effectively constrained by T_{t4}, the entry temperature of the HPT, which is limited by the available material technology level for HPT blades.

These variables are also called static design variables, because they cannot vary at different flight conditions and are fixed for a given engine design.

We also considered two operational variables which can vary the geometry of the engine to better control the engine at individual flight conditions. These two are:

- **Fan IGV**: varying the stator vane angle within the compressor

- **VABI**: it changes the bypass ratio by changing the flow areas at the mixer

We can refer to the above mentioned geometries as dynamic design variables, since they can be adjusted during the flight and therefore they are non-static throughout the mission.

Since it's computationally impossible to analyze every point of the mission envelop, we need to find one critical point where the engine is constrained in some ways. We chose Top of Climb and Subsonic Cruise as our off-design points. For these mission segment we considered:

- **Top of Climb**: a minimum velocity of 1.4 Mach, 50,000 ft of altitude, a climb rate of 800 ft/m and a thrust of 7600 lbf per engine (we consider a fighter with two engines)

- **Subsonic Cruise**: velocity of 0.8 Mach, altitude of 35,000 ft, null climb rate and a 2060 lbf of thrust per engine

After performing six different individual optimization each with a different maximum allowed inlet area for both a VCE and non VCE engine, it is clear how this constraint affects the optimization.

Table 10: *The optimized design variables and performance from each inlet area [26]*

Inlet area [in^2]	$F_{\text{net,SLS}}$ [lbf]	ER_{mixer}	π_{fan}	TFSC$_{\text{Subsonic Climb}}$ [lbm/hr*lbf]	TFSC$_{\text{Top of Climb}}$ [lbm/hr*lbf]
2000	33435	0.942	2.855	0.703	0.882
1900	32873	0.945	2.969	0.712	0.895
1800	32301	0.947	3.103	0.722	0.907
1700	31685	0.954	3.239	0.733	0.921
1600	30818	0.956	3.369	0.745	0.939
1500	30650	0.963	3.630	0.761	0.955

For all six inlet area, both T_{t4} (1777K) and π_{tot} (35.0) were at their upper limit.

As the inlet area gets smaller, the optimizer decrease the design case net thrust. However, since the minimum thrust is still a constraint, the optimizer increases π_{fan} and decreases Bypass Ratio to produce more thrust and reach the minimum required.

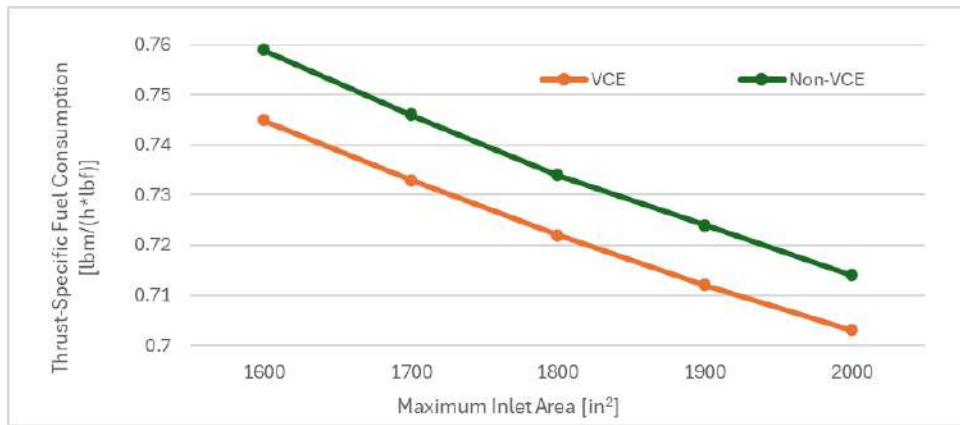As we expected, as the area decreases we also have an increase in TSFC.

Figure 34: *A TSFC comparison between a VCE and a non-VCE engine at Subsonic Cruise [26]*
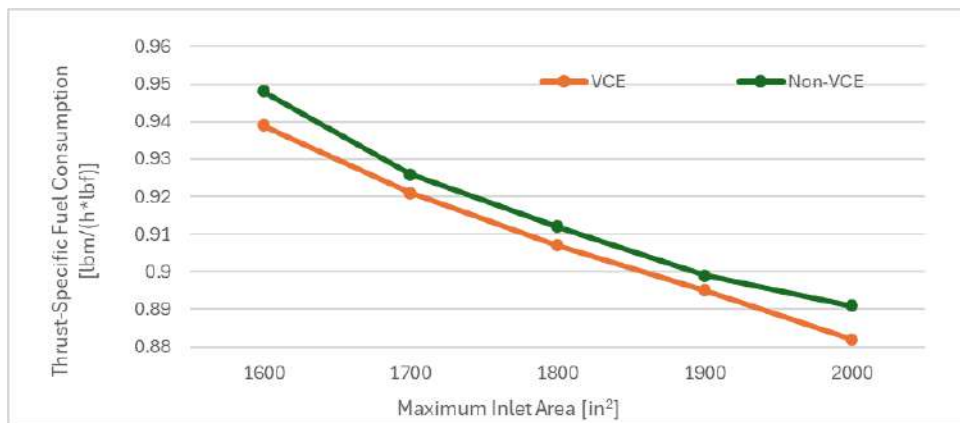

Figure 35: *A TSFC comparison between a VCE and a non-VCE engine at Supersonic Speed [26]*

The 1500 in^2 inlet area was not converging for non-VCE engine and therefore it is not displayed in the graphs.

From *Figure 33* and *Figure 35* it is clear that VCE has more advantages in subsonic cruise rather than in supersonic cruise, even though it still outperforms the non-VCE engine.

If we compare TSFC between the fixed-cycle engine and our VCE we can see how the latter outperforms the non-VCE engine.

Moreover, we can observe having dynamic design variables brings more advantages in subsonic cruise rather than at Supersonic Speed, even if the VCE still have slightly better performance than the fixed cycle engine.

We also performed four single-point optimization to compare its results with the one obtained from the multi-point optimization we have seen in this section. We fixed the inlet area at a medium value (1800 in^2) and we performed the process without considering the performance of any other flight condition other than the design point and the requested flight condition.
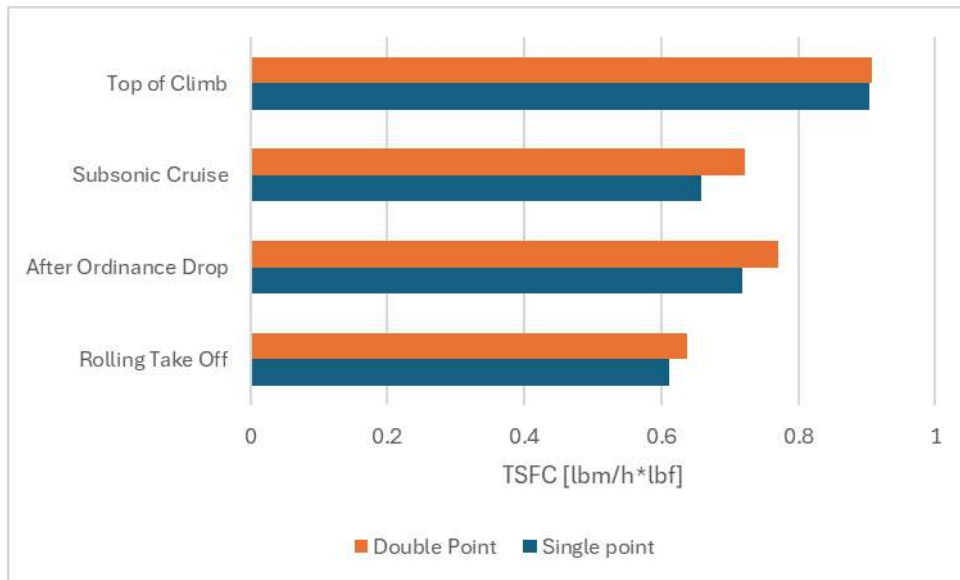
30

Figure 36: *A TSFC comparison between Single and Multi-Point optimization at four different flight conditions [26]*

As we can see from *Figure 36* the single-point optimization outperforms the multi-point optimization in all four flight conditions in terms of TSFC. This difference quantify the sacrifice in fuel consumption efficiency necessary to meet performance demands at different flight conditions. The biggest difference is found at Subsonic Climb with a ratio of 8.6% while the smallest gap is at Top Of Climb with 0.3%.

3.2 The YF-120 for F-22 Raptor

The YF-120 is a Variable Cycle Engine developed from General Electric as the main engine for the ATF (Advanced Tactical Fighter) program. It participated in a fight against the Pratt & Whitney F-120 to power the prototype which would have become the F-22 Raptor, which saw the latter win because of its superior reliability due to its conventional fixed-turbofan architecture [27].
The GE engine had a power of 35,000 lbf (156 kN) wet, and was able to supercruise at a speed of about 1.6 Mach.
It was a twin-spool axial-flow afterburning turbofan, with a two-stage fan driven by a single-stage Low-Pressure Turbine and a five-stage compressor driven by a single-stage High-Pressure Turbine.
The engine has two bypass channels located at the front and rear of the first compressor stage of the high-pressure spool (CDFS), essentials to its Variable Cycle features.
Thanks to his Variable Cycle peculiarity it was more efficient at high altitudes and it could give more specific thrust when required than his opponent (a traditional low-bypass turbofan).
An unexpected disadvantage of the variable system was increased complexity and weight, which forced GE to use simpler pressure driven valves to divert flow rather than complex mechanically actuated valves.

3.3 The GE XA-100 & the P&W XA-101 to upgrade the F-135

ADVENT (Adaptive Versatile Engine Technology) program was an engine development program run by USAF with the goal of developing an efficient Adaptive or Variable Cycle Engine [28]. It was later succeeded by AETD (Adaptive Engine Technology Demonstrator) in 2012 and by AETP (Adaptive Engine Transition Program) in 2016. The latter had the aim of developing a 45,000 lb (200 kN) thrust class ACE to re-engining the F-35 Lightning II.
The results of these campaigns are GE XA-100 and PW XA-101.

3.3.1 The General Electric XA-100

It's a three stream Adaptive Cycle engine, with a fan that can redirect the flow into a third bypass stream in order to augment fuel economy and cooling power.
This engine uses Ceramic Matrix Composites (CMC), a new heat-resistant material that enables higher turbine temperature and therefore more performance. Moreover, the use of these kind of new materials leads also to improvements in

serviceability and reliability of the engine.

GE states [29] that this engine could bring an improvement of more than 20% in acceleration, 30% in range, thanks to the high-efficiency mode, and in thermal management.
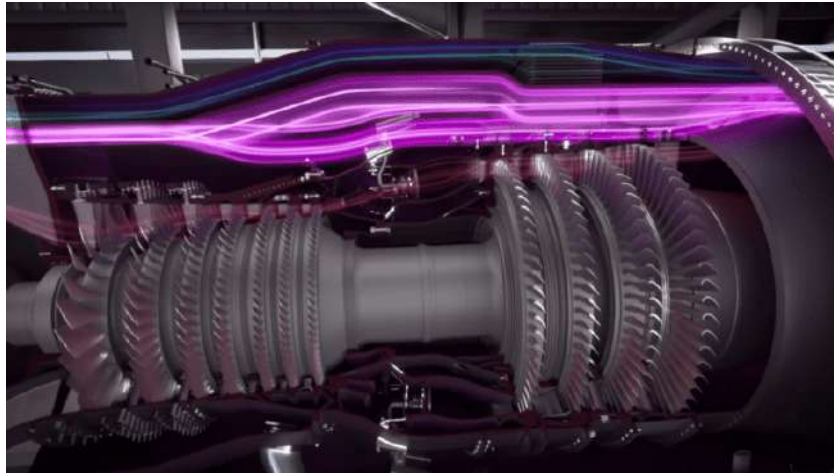

Figure 37: *The General Electric XA-100 ACE [28]*

There have already been successfully conducted four phases of testing and this technology seems to be ready to replace F-135 and power the future of F-35, although this will not happen.

3.3.2 The Pratt & Whitney XA-101

It is the counterpart of Adaptive Cycle Engine from Pratt & Whitney designed to replace F-135.

It seems, like in the past, that PW does not believe too much in this project. As a matter of fact they have pushed to upgrade their F-135 throughout an Engine Core Update. ECU promises to bring good improvements in range, thermal management capacity, thrust and more reliability and durability without overturning the platform, albeit keeping the same engine and upgrading its core [30].

This would be convenient from an economical point of view, and would also reduce the risk of choosing such an advanced and unexplored technology.
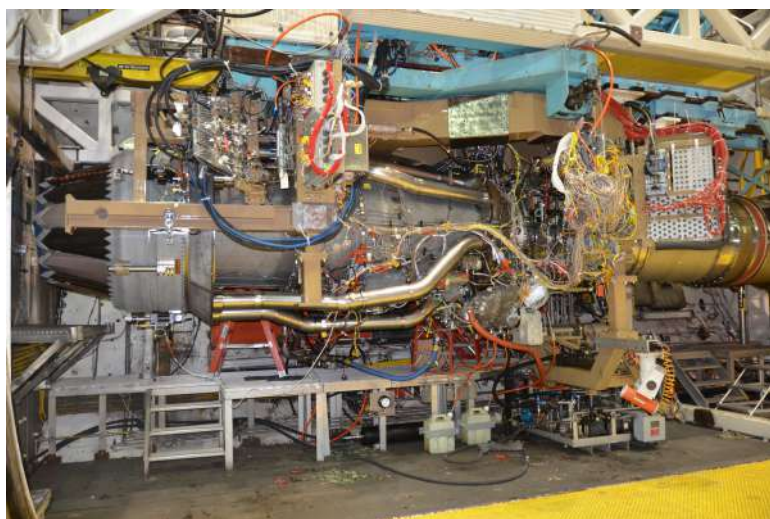

Figure 38: *The Pratt & Whitney XA-101 being tested [31]*

3.4 The GE XA-102 & the PW XA-103 for NGAP

For the Next Generation Air Dominance (NGAD) aircraft, a sixth-generation platform, the request in terms of thrust, range, and thermal capacity are beyond the limits of conventional engines. It is therefore necessary to leave the fixed cycle and develop Adaptive Cycle Engine.

The NGAP (Next Generation Adaptive Propulsion) is the program appointed to reach the above mentioned results. To do so, a new generation of engines needs to be developed. As a matter of fact the new GE XA-102 and PW XA-103 will be developed from their respective predecessor, the XA-100 and XA-101.

At this time, no information is available regarding this next generation engine, albeit one of those two should power the NGAD aircraft for the foreseeable future.

Figure 39: *The Next Generation Air Dominance concept [32]*

Conclusion

The advancements in fighter jet engine technology from the 4th to the 5th generation have profoundly impacted the capabilities and operational effectiveness of modern military aviation. This thesis provided an overall comprehension analysis of these technological steps, showcasing how improvements in materials, digital control systems, and innovative engineering concepts have led to more powerful, efficient, and reliable engines than ever before.

The examination of 4th generation engines revealed a critical transition period in military aviation, where the emphasis shifted towards improving maneuverability, multi-role functionality, and avionics integration. The detailed case studies of engines such as the F-100-PW-229 highlighted the significant enhancements in thrust, reliability, and maintenance.
The EJ-200 is the other 4th generation engine studied in this work. It's a more recent engine with different characteristics compared to the F-100-PW-229: it is lighter and more compact, more efficient and has supercruise capabilities.

The analysis of 5th generation engines demonstrated the remarkable progress achieved in stealth, performance, and adaptability. Engines like the Pratt & Whitney F-119-PW-100 and F-135-PW-100 embody the pinnacle of current aerospace technology, featuring state-of-the-art materials and sophisticated control systems that enable superior performance and operational flexibility.
These capabilities were reached thanks to not only the engine itself, but also by elements correlated to it. As for the F-22 Raptor, caret inlets, S-duct intakes and Minimum Length Nozzles helped the aircraft to reduce both its thermal and noise radar signature.
For what concerns the F-35, caret inlets were left behind to do an additional technological step-forward. With the adoption of Diverterless Supersonic Inlet and Low Observable Axisymmetric Nozzle, stealth capabilities were enhanced while weight and costs were lowered to obtain a better overall performance.

The exploration of the Adaptive Cycle Engine (ACE) underscored its potential to revolutionize future fighter jet propulsion. By offering the ability to switch between different operational modes, the ACE can optimize performance for various mission profiles, enhancing fuel efficiency, thrust, and overall effectiveness.
The adoption of ACE brings with it big improvements also in flow control, which reduces the inlet spillage drag and thus improve performance.
Another important field in which research should be conducted is optimization. In this work we compared a single-point optimization process with a multi-point one. We observed how the latter brought better performance and big improvements in terms of adaptability to a wider range of flight conditions compared to the single-point optimization.
The feasibility study and comparative analysis presented in this thesis highlight the improvements and advantages that ACE can bring to future military aircraft, albeit at the same time the adoption of these high-technology engines leads to many problems as high research and design costs together with mechanical and weight limitations.
Data given by engine manufactures presents huge improvements in range, thrust, and fuel consumption. When reading these reports we need to be critical and try to evaluate the distribution of improvements. Part of them are associated to the adoption of a variable architecture, while the remainder is related to further development in materials, controls and other engineering innovations.

In conclusion, the advancements in fighter jet engine technology analyzed in this thesis have illustrated the dynamic and innovative nature of military fighter jets [33]. As the industry continues to evolve, present and future engines will need to meet the ever-increasing demands of modern warfare, ensuring that military aircraft remain at the forefront of technological capability and operational effectiveness.

References

1. H. Roger, D.G. Mitchell, *Flying Qualities of Relaxed Static Stability Aircraft - Volume I: Flying Qualities Airworthiness Assessment and Flight Testing of Augmented Aircraft, 1983*

2. *https://www.prattwhitney.com/en/products/military-engines/f100*

3. Pictures, *https://en.wikipedia.org/wiki/North_American_F-100_Super_Sabre*

4. B.L. Koff, *F100-PW-229 Higher Thrust in Same Frame Size, 1989*

5. *https://aeroreport.de/en/aviation/blisk-development-how-blade-and-disk-became-one*

6. *https://www.mtu.de/engines/military-aircraft-engines/fighter-aircraft/ej200/*

7. Pictures, *https://en.wikipedia.org/wiki/Eurojet_EJ200*

8. *5th Generation Fighters. Lockheed Martin, 2010*

9. D.C. Aronstein, M.J. Hirschberg, A.C. Piccirillo, *Advanced Tactical Fighter to F-22 Raptor: Origins of the 21st Century Air Dominance Fighter, 1998*

10. *Forecast International, Aviation Gas Turbine Forecast, Pratt & Whitney F119, 2012*

11. *https://www.baesystems.com/en-us/definition/what-is-fadec*

12. R.O Bura, M.H. Askary, H.J Bagus, *Numerical Simulations of Flow Separation In Over-Expanded Supersonic Nozzle With Rectangular Cross Section, 2009*

13. S.S Lin, Y.W. Liu, M.C. Shen, B.J. Tsai, *Design of Hypersonic Waverider with Wing-Body-Tail-Inlet-Engine, 1996*

14. Pictures, *https://en.wikipedia.org/wiki/Pratt_%26_Whitney_F135*

15. *Pratt & Whitney, F135 Specs Carts*

16. K. Mehrab, Z. Alama, S.T. Haque, *Comparison and Development Analysis of F119-PW-100 & F135-PW-100*

17. C. Wiegand, B.A. Bullick, J.A. Catt, J.W. Hamstra, G.P. Walker, S. Wurth, *F-35 Air Vehicle Technology Overview, 2018*

18. *https://www.prattwhitney.com/fr/products/military-engines/f135*

19. A. Hasselrot, B. Montogomerie, *An Overview of Propulsion Systems for Flying Vehicles, 2005*

20. H. Aygun, M. Emin, I. Ekmekci, *Energy and Performance Optimization of an Adaptive Cycle Engine for Next Generation Combat Aircraft, 2020*

21. X. Meng, Z. Zhu, M. Chen, *Performance Optimization of Adaptive Cycle Engine during Subsonic Climb, 2019*

22. H.R. Patel, D.R. Wilson, *Parametric Cycle Analysis of Adaptive Cycle Engine, 2018*

23. M. Chen, J. Zhang, H. Tang, *Performance Analysis of a Three-Stream Adaptive Cycle Engine during Throttling, 2018*

24. X. Meng, Z. Zhu, *Steady-State Performance Comparison of Two Different Adaptive Cycle Engine Configurations, 2017*

25. Y. Xu, M, Chen, H. Tang, *Preliminary Design Analysis of Core-Driven Fan Stage in Adaptive Cycle Engine, 2019*

26. J.P. Jasa, J.S. Gray, J.A. Siedel, C.A. MAder, J.R.R.A. Martins, *Multi-point Variable Cycle Engine Design Using Gradient-based Optimization, 2019*

27. *GE F120 Powerplant Uses Fan Bypass Door to Regulate Variable Cycle (1990). Aviation Week and Space Technology. 30 Jul 1990. Vol. 133, No. 5; pg. 21*

28. *https://www.ge.com/news/press-releases/testing-on-ges-first-xa100-adaptive-cycle-engine-concludes-proves-out*

29. *https://www.geaerospace.com/military-defense/engines/xa100*

30. *https://www.prattwhitney.com/en/products/military-engines/f135/engine-core-upgrade*

31. Pictures, *https://en.wikipedia.org/wiki/Pratt_%26_Whitney_XA101*

32. Pictures, *https://en.wikipedia.org/wiki/Next_Generation_Air_Dominance*

33. O. Younossi, M.V. Arena, R.M. Moore, M. Lorell, J. Mason, J.C. Graser for United States Air Force, *Military Jet Engine Acquisition, Technology Basics and Cost-Estimating Methodology, 2002*

34. J. Zhang, H. Tang, M. Chen, *Robust Design of an Adaptive Cycle Engine Performance under Component Performance Uncertainty, 2021*